Available online at www.sciencedirect.com

ScienceDirect

Geochimica et Cosmochimica Acta 224 (2018) 132–153

Geochimica et Cosmochimica Acta

www.elsevier.com/locate/gca

Reworking of Archean mantle in the NE Siberian craton by carbonatite and silicate melt metasomatism: Evidence from a carbonate-bearing, dunite-to-websterite xenolith suite from the Obnazhennaya kimberlite

Dmitri A. Ionov [a,b,*], Luc S. Doucet [c,d], Yigang Xu [b], Alexander V. Golovin [e,f], Oleg B. Oleinikov [g]

[a] *Géosciences Montpellier, Université de Montpellier, 34095 Montpellier, France*
[b] *Guangzhou Institute of Geochemistry, Chinese Academy of Sciences, 510640 Guangzhou, China*
[c] *Laboratoire G-Time, Université Libre de Bruxelles, 1000 Brussels, Belgium*
[d] *The Institute of Geosciences Research, Department of Applied Geology, Curtin University, Perth 6845, Australia*
[e] *Sobolev Institute of Geology and Mineralogy, Siberian Branch Russian Academy of Sciences, Koptyuga 3, Novosibirsk 630090, Russian Federation*
[f] *Novosibirsk State University, Pirogova 2, Novosibirsk 630090, Russian Federation*
[g] *Diamond and Precious Metal Geology Institute, Siberian Branch Russian Academy of Sciences, Lenina 39, Yakutsk 677007, Russian Federation*

Received 18 August 2017; accepted in revised form 30 December 2017; available online 10 January 2018

Abstract

The Obnazhennaya kimberlite in the NE Siberian craton hosts a most unusual cratonic xenolith suite, with common rocks rich in pyroxenes and garnet, and no sheared peridotites. We report petrographic and chemical data for whole rocks (WR) and minerals of 20 spinel and garnet peridotites from Obnazhennaya with Re-depletion Os isotope ages of 1.8–2.9 Ga (Ionov et al., 2015a) as well as 2 pyroxenites. The garnet-bearing rocks equilibrated at 1.6–2.8 GPa and 710–1050 °C. Some xenoliths contain vermicular spinel-pyroxene aggregates with REE patterns in clinopyroxene mimicking those of garnet. The peridotites show significant scatter of Mg# (0.888–0.924), Cr_2O_3 (0.2–1.4 wt.%) and high NiO (0.3–0.4 wt.%). None are pristine melting residues. Low-CaO-Al_2O_3 ($\leq$0.9 wt.%) dunites and harzburgites are melt-channel materials. Peridotites with low to moderate Al_2O_3 (0.4–1.8 wt.%) usually have CaO > Al_2O_3, and some have pockets of calcite texturally equilibrated with olivine and garnet. Such carbonates, exceptional in mantle xenoliths and reported here for the first time for the Siberian mantle, provide direct evidence for modal makeover and Ca and LREE enrichments by ephemeral carbonate-rich melts. Peridotites rich in CaO and Al_2O_3 (2.7–8.0 wt.%) formed by reaction with silicate melts.

We infer that the mantle lithosphere beneath Obnazhennaya, initially formed in the Mesoarchean, has been profoundly modified. Pervasive inter-granular percolation of highly mobile and reactive carbonate-rich liquids may have reduced the strength of the mantle lithosphere leading the way for reworking by silicate melts. The latest events before the kimberlite eruption were the formation of the carbonate-phlogopite pockets, fine-grained pyroxenite veins and spinel-pyroxene symplectites. The reworked lithospheric sections are preserved at Obnazhennaya, but similar processes could erode lithospheric roots in the SE Siberian craton (Tok) and the North China craton, where ancient melting residues and reworked garnet-bearing peridotites are absent.

The modal, chemical and Os-isotope compositions of the Obnazhennaya xenoliths produced by reaction of refractory peridotites with melts are very particular (high Ca/Al, no Mg#-Al correlations, highly variable Cr, low $^{187}Os/^{188}Os$, continuous

* Corresponding author at: Géosciences Montpellier, Université de Montpellier, 34095 Montpellier, France.
E-mail address: dmitri.ionov@gm.univ-montp2.fr (D.A. Ionov).

https://doi.org/10.1016/j.gca.2017.12.028

modal range from olivine-rich to low-olivine peridotites, wehrlites and websterites) and distinct from those of fertile lherzolites in off-craton xenoliths and peridotite massifs. These features argue against the concept of 'refertilization' of cratonic and other refractory peridotites by mantle-derived melts as a major mechanism to form fertile to moderately depleted lherzolites in continental lithosphere. The Obnazhennaya xenoliths represent a natural rock series produced by 'refertilization', but include no rocks equivalent in modal, major and trace element to the fertile lherzolites. This study shows that 'refertilization' yields broad, continuous ranges of modal and chemical compositions with common wehrlites and websterites that are rare among off-craton xenoliths.

Keywords: Lithospheric mantle; Siberian craton; Xenolith; Garnet peridotite; Pyroxenite; Carbonate; Metasomatism

1. INTRODUCTION

Cratons are the oldest continental domains on Earth. Their longevity and stability are usually attributed to the protective presence of thick lithospheric 'roots' mainly composed of refractory harzburgites that experienced extensive removal of partial melt at high pressure (P) to produce high Mg# [molar Mg/(Mg + Fe)] and very low Ca and Al in the residues (Walter, 1999; Herzberg, 2004). Together with low temperatures (T), this makes cratonic harzburgites less dense and more buoyant and strong than the asthenosphere made up of fertile peridotites (e.g. Boyd and McCallister, 1976). Yet, many cratonic peridotite xenoliths are deformed (sheared), and show enrichments in Fe, Ca and Al attributed to metasomatism by migrating melts, which may reduce their strength and buoyancy. A growing body of evidence indicates that cratonic roots may suffer erosion and rejuvenation (Foley, 2008) ranging from thinning and replacement of their deepest portions, like in Wyoming (Humphreys et al., 2015; Snyder et al., 2017) and Tanzania (Wölbern et al., 2012), to more or less complete removal (delamination) of lithospheric mantle, e.g. as evoked for the North China craton (Fan et al., 2000; Xu, 2001) or parts of the Siberian craton (Ionov et al., 2006a; Moyen et al., 2017).

The reasons for erosion, re-working and destruction of cratonic roots may ultimately reside in mantle convection, global-scale geodynamic processes and supercontinent cycles. In detail, the evolution of cratonic roots has been attributed to mechanical, thermal and/or chemical action of asthenospheric upwelling and mantle plumes (or even super-plumes, e.g. Howarth et al. (2014)), lithospheric extension and subduction accompanied by intrusion of carbonatite or silicate melts or fluids (e.g. Foley, 2008; Liu et al., 2016). However, the mechanisms of these processes remain poorly understood (e.g. Fan et al., 2000; Gao et al., 2008). They can be elucidated using xenolith suites from domains where lithospheric erosion was incomplete, that both preserve relics of refractory mantle and show its transformation stages, but such suites are rare (Foley, 2008; Wang et al., 2015).

Xenoliths hosted by the Obnazhennaya kimberlite in the NE Siberian craton may be one of such suites. Early studies by Russian geologists (see summaries in Ukhanov et al., 1988; Spetsius and Serenko, 1990) found that it is dominated by low-olivine peridotites and various pyroxenites and includes eclogites, but found no diamonds, no sheared peridotites, and few coarse garnet harzburgites, unlike for kimberlites from the central craton (Sobolev, 1977). While the eclogites have been relatively well studied (Snyder et al., 1997; Taylor et al., 2003), only scarce and partial data on peridotites and pyroxenites have been published in the international literature. It appears that the base of the lithosphere at Obnazhennaya is much more shallow than in the central Siberian craton (<4 GPa vs. 6–7 GPa) (Howarth et al., 2014).

Ionov et al. (2015a) reported Re-Os isotope and PGE analyses for 19 spinel and garnet peridotites and established that the mantle lithosphere beneath Obnazhennaya formed in two stages, at 2.6–2.9 Ga and ~2 Ga, based on Re-depletion model ages for refractory rocks. Pernet-Fisher et al. (2015) provided Re-Os and PGE analyses of 'bulk' materials from two Obnazhennaya xenoliths, as well as for six olivine separates, all from apparently very small xenoliths. They yielded an extremely broad γO_{ch} range (−10 to +159), whose meaning is not clear. Howarth et al. (2014) published in-situ major and trace element analyses of minerals in these samples, but no whole-rock or modal compositions.

We report petrographic observations, modal abundances and whole rock (WR) and mineral major and trace element compositions for 20 peridotite and two pyroxenite xenoliths from Obnazhennaya. Re-Os isotope and PGE data for 19 samples in this study were provided by Ionov et al. (2015a). We show that the Obnazhennaya xenolith suite is different from that in the well-studied Udachnaya kimberlite in the central Siberian craton, and from many cratonic xenolith suites elsewhere. In particular it contains few, if any, pristine melting residues, and mainly includes rocks formed by reaction of such residues with migrating melts. We examine media and processes that could cause widespread re-working of the mantle lithosphere beneath Obnazhennaya and possibly affect other cratonic and off-craton mantle domains.

2. GEOLOGIC SETTING AND SAMPLES

2.1. Geologic setting and mantle xenoliths

The Siberian craton located in the center of Siberia, Russia (Fig. 1; KML map), mainly within the Sakha (Yakutia) autonomous republic, is one of the largest contiguous Archean to Paleoproterozoic continental domains on Earth (Pearson and Wittig, 2008). The crustal basement

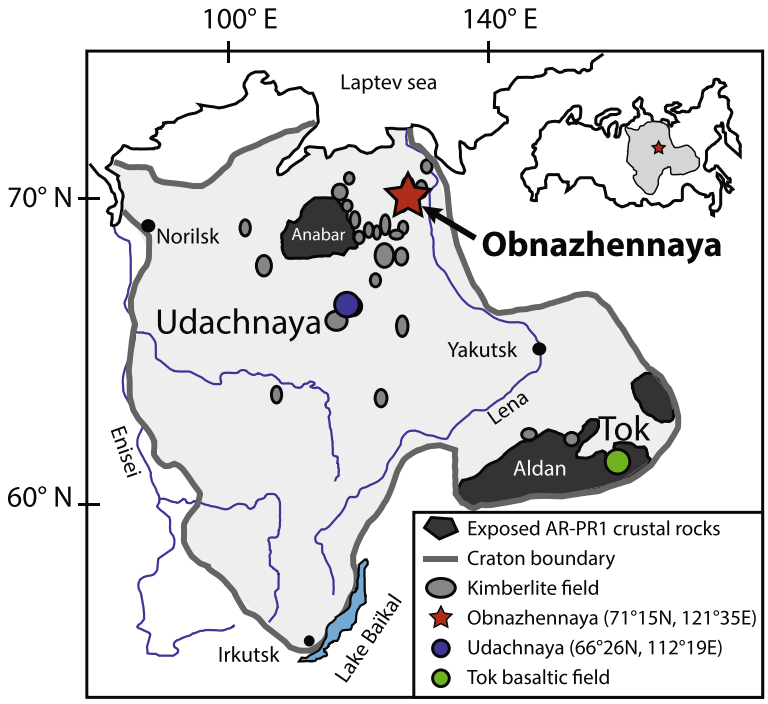

Fig. 1. Locality map for the Obnazhennaya (red star) and Udachnaya kimberlite pipes, and the Tok basaltic field in the Siberian craton; the inset in the upper right shows the position of the craton in the Russian Federation. Also shown are the Anabar and Aldan shields and major kimberlite fields. (For interpretation of the references to colour in this figure legend, the reader is referred to the web version of this article.)

rocks are exposed mainly on the Anabar (e.g. Paquette et al., 2017) and Aldan shields (Fig. 1), while much of the rest is hidden under a thick sedimentary and volcanic cover. The crustal rocks are punctured by Paleo- to Mesozoic kimberlite pipes, located mainly in a belt extending from the central to NE craton (Sobolev, 1977), and by Cenozoic alkali basaltic volcanoes near its SE margin (Ionov et al., 2005c) (Fig. 1).

The Obnazhennaya pipe (70°15′N, 121°35′E) is located in the NE craton (Fig. 1), and belongs to the Middle-Late Jurassic Kuoyka (Kuoika) kimberlite field that carries almost no diamonds. The kimberlitic breccia cutting flat-lying Meso- to Neoproterozoic (0.8–1.4 Ga) sediments is exposed on the bank of the Olenek River near its confluence with the Kuoyka River (Obnazhennaya means exposed in Russian). It has been dated at 157 ± 2 Ma from Rb-Sr data (Agashev et al., 2004) and 168 ± 11 Ma from paleomagnetic data (Blanco et al., 2013), while U-Pb ages on zircon and perovskite from other pipes in the Kuoyka field range from 128 to 170 Ma (Davis et al., 1980; Kinny et al., 1997; Griffin et al., 1999).

Studies of mantle xenoliths from Obnazhennaya published in the 1970–80s in Russian noted a large proportion of garnet pyroxenites and eclogites, common development of late-stage garnet and pyroxenes in peridotites, the absence of deformed peridotites and of high-P-T rocks, and suggested that the mantle lithosphere is only 120–130 km thick (e.g. Sobolev, 1977; Ukhanov et al., 1988; Spetsius and Serenko, 1990). As noted in the previous section, very little data on peridotite xenoliths from Obnazhennaya are available in the international literature, in particular, no full bulk rock chemical analyses. Taylor et al. (2003) and Howarth et al. (2014) reported a P-T range of 1.4–4.2 GPa and 620–1100 °C for olivine-bearing and eclogitic xenoliths from Obnazhennaya.

2.2. Sample selection and preparation

The 22 xenoliths in this study, for which we report comprehensive analytical results, are listed in Table 1 that provides a summary of essential petrologic and chemical data on each sample (see also Table S1 of Appendix 1). They were selected from a larger collection to: (a) represent major peridotite types found as xenoliths in the Obnazhennaya kimberlite, and (b) provide ≥100 g of material for WR powders. Preference is given to refractory (olivine-rich, pyroxene-poor) rocks likely to be residues of melt extraction. They include 19 samples analyzed for Os isotopes and PGE by Ionov et al. (2015a) plus three Ca-Al-rich peridotites and pyroxenites. We also report mineral analyses (Appendix 1) and petrographic observations (Appendix 2) for several other Obnazhennaya xenoliths.

The xenoliths are 10–30 cm in size. Their rinds were removed by sawing. Slabs of fresh material from xenolith cores were inspected to make sure they contain no kimberlite, veins or modal gradations. A large amount of fresh material (normally >100 g) was taken to provide representative WR samples taking into account mineral grain size (Boyd, 1989) and crushed to <5–10 mm in a steel jaw crusher carefully cleaned to avoid cross-contamination.

Table 1
Summary of essential petrologic and geochemical data on samples in this study.

Sa. N°	Rock type	T, °C	P, GPa	Whole-rock composition, wt.%				Ol	Spl	Modal composition, %									Re-Os
		Ca-opx	NG85	Al_2O_3	CaO	Cr_2O_3	Mg#	Mg#	Cr#	Ol	Opx	Cpx	Sp	Gar	Phl	Carb	Amph	Pl	T_{RD}, Ga
Low-Ca-Al dunites and harzburgites																			
Obn 41-13	Sp Hz, protogr.	933	/1.5/	0.82	0.70	0.55	0.919	0.923	0.14	69.8	27.3	2.2	0.7	–	–	–	–	–	2.3
Obn 59-13	Sp Dunite	–	–	0.14	0.38	0.18	0.915	0.916	0.52	98.2	–	1.5	0.4	–	–	–	–	–	1.7
Obn 60-13	Sp-rich Dunite	–	–	0.93	0.63	1.41	0.888	0.892	0.53	94.4	–	2.2	3.3	–	–	–	–	–	/1.2/
Obn 69-13	Sp Hz	923	/1.5/	0.76	0.33	0.43	0.918	0.921	0.43	74.8	23.8	0.7	0.7	–	–	–	–	–	1.7
Phl-bearing, mainly carbonate bearing, Ca-rich peridotites with low to moderate Al																			
Obn 08-13	Gar-Sp-Phl Hz	729	2.1	1.20	2.77	0.41	0.919	0.921	0.58	69.9	20.4	0.8	0.5	2.3	1.6	4.4	–	–	1.8
Obn 22-13	Sp Hz, vermicular	1027	/1.5/	1.82	2.20	1.06	0.917	0.920	0.36	76.1	15.8	1.9	2.6	–	0.5	3.1	–	–	2.7
Obn 24-13	Sp-Phl Lh	784	/1.5/	0.41	2.44	0.19	0.918	0.920	0.94	84.2	6.6	3.6	0.1	–	2.4	3.1[a]	–	–	2.9
Obn 39-13	Gar-Sp Hz	711	1.6	1.90	3.17	0.87	0.918	0.920	0.59	66.4	20.7	2.1	1.3	4.0	1.1	4.5	–	–	2.2
Obn 53-13	Gar-Sp-Phl Hz	767	2.6	1.42	3.22	1.05	0.919	0.924	0.63	75.7	12.0	0.5	1.7	2.9	1.8	5.4	–	–	2.8
Ca-rich peridotites with low to moderate Al																			
Obn 01-13	Amph-Sp Lh	772	/1.5/	1.68	1.40	0.63	0.917	0.916	0.37	58.3	33.7	4.0	1.2	–	–	–	2.8	–	2.0
Obn 12-13	Sp Lh-Wh, vermic.	1047	/1.5/	1.63	2.44	1.04	0.920	0.921	0.39	84.0	2.6	10.7	2.6	–	–	–	–	–	2.0
Obn 37-13	Sp Lh-Wh	685	/1.5/	0.57	2.48	0.18	0.915	0.918	0.33	85.2	3.9	10.5	0.4	–	–	–	–	–	2.6
Obn 68-13	Sp Wh	891	/1.5/	0.88	2.94	0.51	0.909	0.912	0.40	84.0	2.5	12.4	1.2	–	–	–	–	–	1.9
O–1017	Sp Lh	706	/1.5/	1.10	2.50	0.45	0.917	0.923	0.55	74.8	13.0	11.2	1.0	–	–	–	–	–	2.8
O-1061	Gar-Sp Hz protogr.	716	/1.5/	0.82	1.95	0.49	0.916	0.919	0.42	87.7	2.6	4.2	1.3	4.2	–	–	–	–	2.9
Ca,Al–rich lherzolites																			
Obn 06-13	Sp Lh, protogr.	668	/1.5/	3.25	4.86	0.95	0.924	0.924	0.21	68.7	5.7	21.7	4.0	–	–	–	–	–	/1.6/
Obn 20-13	Sp Lh, protogr.	678	/1.5/	3.22	3.24	1.01	0.920	0.923	0.23	60.2	21.5	14.5	3.8	–	–	–	–	–	/1.6/
Obn 21–13	Gar-Sp Lh	698	2.0	7.98	5.49	1.31	0.900	0.922	0.33	44.7	7.0	17.4	1.1	29.8	–	–	–	–	n.a.
Obn 49–13	Gar Lh	753	2.8	3.40	3.46	0.46	0.907	0.915	-	67.8	6.3	13.4	-	12.4					
O-47	Sp Lh	–	–	2.66	3.76	0.41	0.909	0.908	n.a.	61.8	22.0	16.2	n.a.	–	–	–	–	–	1.8
Garnet and plagioclase pyroxenites																			
Obn 58-13	Sp-Pl Wbst vein	–	–	11.08	3.22	0.40	0.919	–	0.03	–	28.9	59.1	7.6	–	–	–	–	4.5	
O-1080	Ol-Gar-Sp Wbst	729	2.1	7.18	8.02	1.42	0.909	0.922	0.40	30.1	12.6	38.1	1.3	17.9	–	–	–	–	

Ol, olivine; Opx, orthopyroxene; Cpx, clinopyroxene; Sp, spinel; Gar, garnet; Carb, carbonate (calcite); Amph, amphibole; Phl, phlogopite; Pl, plagioclase.
Lh, lherzolite; Hz, harzburgite; Wh, wehrlite; Wbst, websterite; protogr., protogranular microstructure; vermic., vermicular pyroxene-spinel aggregates; n.a., not available; –, absent.
Equilibration temperatures (T) estimated with the Ca-in-opx method of Brey and Köhler (1990) modified by Nimis and Grütter (2010), and assuming P = 1.5 GPa for spinel peridotites.
Equilibration pressures (P) for gar-bearing rocks estimated with the opx-gar barometer of Nickel and Green (1985); values in brackets /1.5/ used for T estimates for spinel peridotites.
Modal estimates obtained by least squares method from whole-rock and mineral analyses, and normalized to 100%. Sample 58-13 is a vein in a harzburgite.
Re-depletion model Os-isotope ages are from Ionov et al. (2015a), values in brackets are not robust because of high Al_2O_3 or low Mg#.
Some chemical and modal data in this table were previously reported in Ionov et al. (2015a).
[a] Modal carbonate in sample 24-13 is an estimate for calcite component that could react with host peridotite to yield metasomatic Cpx-Spl ± Phl pockets.

Splits of crushed material (50–100 g) were ground to fine powder in agate. The mass of the material crushed to obtain WR samples is given in Table S2 of Appendix 1.

3. MATERIALS AND ANALYTICAL METHODS

The concentrations of major and minor elements in 22 WR samples were determined by wavelength-dispersive (WD) X-ray fluorescence (XRF) spectrometry at J. Gutenberg University, Mainz. The rock powders were ignited for ≥3 h at 1000 °C to turn all FeO into Fe_2O_3 and expel volatiles before the analyses; Fe_2O_3 concentrations were recalculated to FeO, the prevalent form of iron in mantle peridotites. Glass beads, produced by fusing 1 g of ignited powders with 5 g of dried LiB_4O_7 (1:6 dilution) were analyzed on an X-ray sequential spectrometer Philips MagiX Pro using ultramafic and mafic reference samples as external standards. Reference sample JP-1 was analyzed twice as unknown together with the samples for quality control with results close to recommended values (Table S2 of Appendix 1). This low-dilution bead technique was earlier shown to yield improved accuracy and precision compared to conventional XRF analyses judging from reproducibility of duplicates, analyses of reference materials as unknowns and less scatter on element co-variation plots (Ionov et al., 2005a; Ionov, 2007; Ionov and Hofmann, 2007).

Major element compositions of minerals (Table S3 of Appendix 1) were obtained by WD electron probe microanalysis (EPMA) at "Service Microsonde Sud", Université de Montpellier (UM) on a Cameca SX-100 using 15 kV, 15 nA current and counting times of 20–60 s for peaks and background; standards were natural and synthetic minerals. Concentrations were obtained from raw intensities using the "X-PHI" quantification procedure (Merlet, 1994). The major minerals were mainly analyzed in grain mounts. Selected samples were also run in thin sections to evaluate heterogeneities and zoning of mineral grains, and in particular to analyze fine-grained minerals, e.g. metasomatic carbonates, mica and late-stage clinopyroxene (cpx). Modal abundances were estimated from major oxide compositions of bulk rocks and minerals with least square method (Table 1).

Whole-rock trace element compositions were determined by inductively coupled plasma mass-spectrometry (ICPMS) at the UM following a modified method of Ionov et al. (1992). Finely ground rock powders (100 mg) were dissolved in HF-$HClO_4$ mixtures. Dried samples were taken up in HNO_3 and diluted in 2% HNO_3 to 1:2000 shortly before the analysis. The sample solutions were analyzed on an Element XR instrument together with synthetic calibration solutions, blanks and 3 reference materials (RM: BEN, UBN and JP-1) analyzed as unknowns for control. Full procedural blanks are 0.07 ppm for Ba, 0.01–0.03 ppm for Sr, ~0.001–0.003 ppm for Rb, Y, Zr, Nb, Cs, La, Ce, Hf, Th, and <0.001 ppm for other rare earth elements (REE), Ta and U (Table 4S of Appendix 1).

Garnet and cpx were analyzed for trace elements by laser-ablation (LA) ICPMS at the UM mainly in grain mounts as well as in polished sections. The Element XR ICPMS instrument was coupled with UV (193 nm) Excimer CompEx 102 laser on an GeoLas Q+ platform. The laser was operated at 8 Hz, ~12 mJ cm^{-2} pulse energy and a beam size of 70 μm. Helium was used as carrier gas. Acquisition time was 60 s for signal and 90 s for background. The NIST 612 RM was used as external standard (Pearce et al., 1997), the BIR-1g RM measured with the minerals for quality control (Table 5S of Appendix 1) yielded consistent results. Data reduction was done with the GLITTER software (van Achterbergh et al., 2001).

4. RESULTS

4.1. Petrography

4.1.1. Rock types and microstructures

Scanned thin section images of samples in this study are provided in Appendix 2. Out of 22 xenoliths listed in Table 1 seven contain garnet including one garnet lherzolite and six garnet-spinel harzburgites, lherzolites and olivine websterites (Streckeisen, 1976). Fourteen samples (dunites, harzburgites and lherzolites) contain spinel, but no garnet. The peridotites have protogranular to mosaic-equigranular microstructures (Mercier and Nicolas, 1975) and are coarse to medium grained, except for fine-grained spinel peridotites Obn 63-13 and 68-13. Alteration products are present in some rocks, mainly serpentine at grain boundaries and veins in olivine; locally they contain fine-grained carbonates and phlogopite (phl).

The xenoliths are grouped into four series (Table 1). The first one consists of four cpx-poor spinel peridotites: two dunites that contain no orthopyroxene (opx) and two opx-rich harzburgites. The second and third series, with a total of 11 samples, combine peridotites with low to moderate total abundances of cpx ± garnet ± amphibole. Among them, five xenoliths are identified as a specific group because they are the only samples in this study that contain carbonates and/or phl texturally equilibrated with garnet and olivine (Fig. 2a). The fourth series has eight samples rich in pyroxenes ± garnet (6 lherzolites, 2 pyroxenites); such rocks are common among Obnazhennaya xenoliths.

Characteristic features of the Obnazhennaya suite are the rarity of harzburgites (most common rock type for kimberlite-hosted xenoliths) and the absence of compositional gaps between fertile garnet lherzolites, olivine-bearing and olivine-free garnet pyroxenites, with apparently continuous modal variations of olivine, pyroxenes and garnet between these rock types. Also common are low opx abundances in peridotites, e.g. in lherzolites transitional to wehrlites (Table 1). In some of these rocks, opx is replaced with interstitial cpx that contains inclusions of opx, garnet and olivine (Fig. 3a and c), or with fine-grained mosaic aggregates of cpx and olivine ± phl (Obn 24-13) or amphibole (Obn 01-13).

Garnet usually coexists with spinel, often as vermicular intergrowths (Figs. 2a and 4a). Several peridotites have much higher modal spinel (2.5–4%) than is common for fertile or refractory mantle peridotites (e.g. Ionov, 2007; Doucet et al., 2012; Pearson et al., 2014). Spinel morphology ranges from euhedral in dunite Obn 60-13 to a range of anhedral shapes.

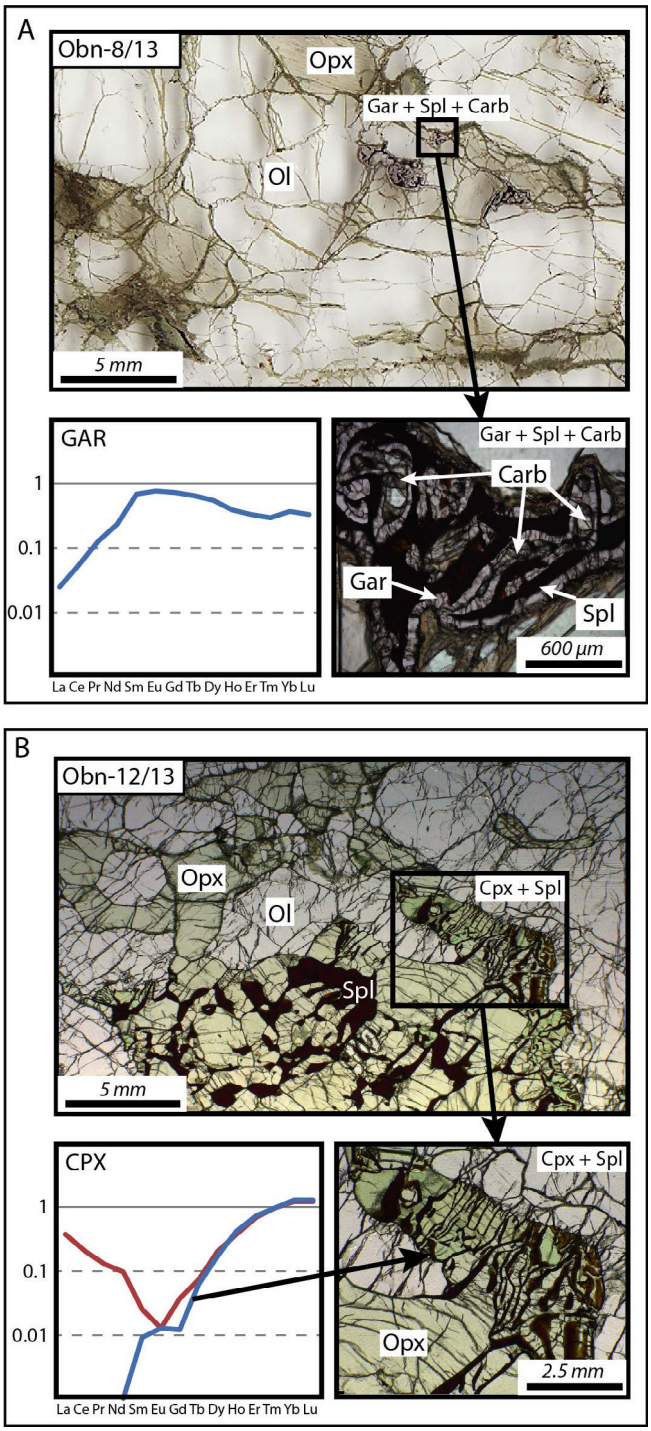

Fig. 2. Photomicrographs of two Obnazhennaya peridotite xenoliths in transmitted plane-polarized light, and typical primitive mantle-normalized (McDonough and Sun, 1995) rare earth element (REE) mineral patterns. Abbreviations: Ol, olivine; Opx, orthopyroxene; Cpx, clinopyroxene; Gar, garnet; Spl, spinel; Carb, carbonate. A. Obn 8-13 (carbonate-bearing, Ca-rich harzburgite with moderate Al). Top, position of Carb-Gar-Ol-Spl clusters in coarse-grained harzburgite; bottom right, a close view of a Carb-Gar-Ol-Spl cluster showing textural equilibration of carbonate with olivine and garnet; bottom left, garnet REE pattern is humped and slightly sinusoidal due to the enrichment in medium REE related to carbonate formation. B. Obn 12-13 (Ca-rich peridotite with moderate Al). Top, homogeneous pyroxenes (top left) coexisting with composite, vermicular pyroxene-spinel aggregates probably formed by garnet breakdown; bottom right, a close view of a Cpx grain with sub-parallel vermicular spinel inclusions; bottom left, the REE pattern of the Cpx from the center of the grain (blue) is typical of unmetasomatized garnet, from which it was apparently formed; the rim pattern (red) is enriched in light REE due to late-stage metasomatism. (For interpretation of the references to colour in this figure legend, the reader is referred to the web version of this article.)

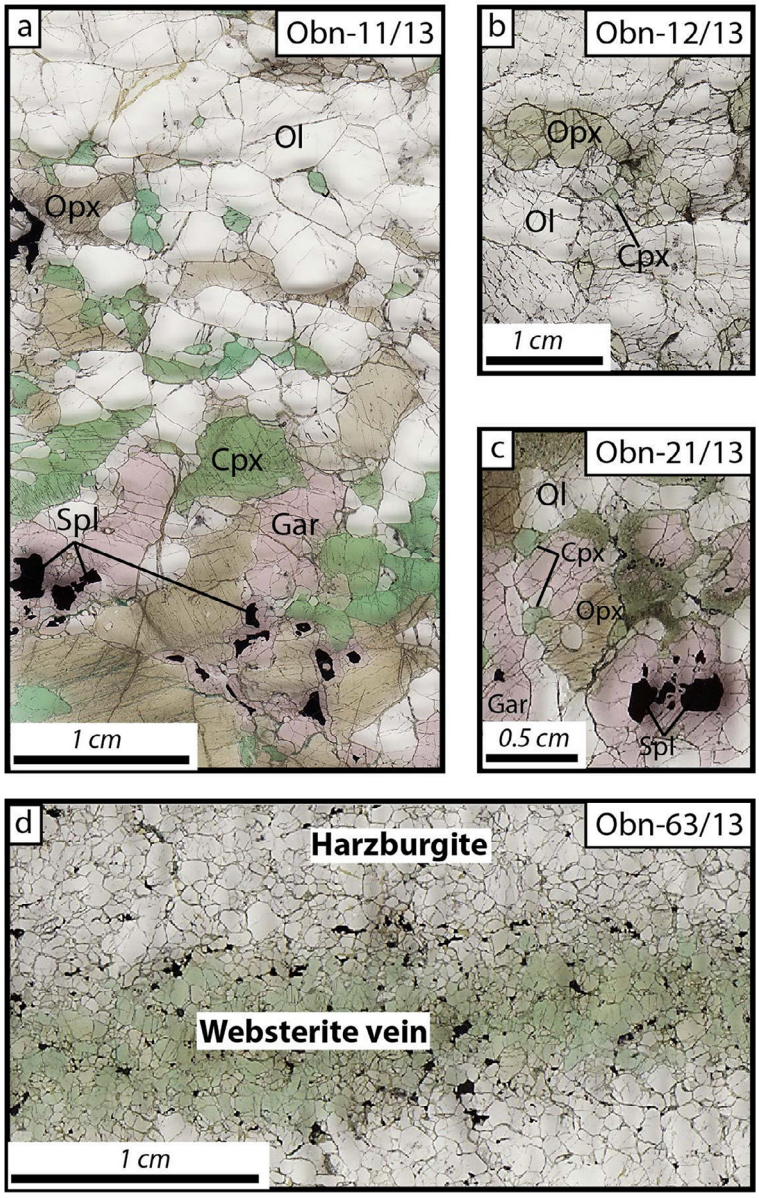

Fig. 3. Photomicrographs of representative Obnazhennaya xenoliths in transmitted light; abbreviations are the same as in Fig. 2. (a) A full-size section of composite xenolith Obn 11-13 with continuous gradation from harzburgite (top) to spinel lherzolite (upper middle), Ol-Gar-Spl websterite (lower middle) and Ol-free websterite (bottom left) over a distance of ~5 cm. The olivine-rich side of the section consists of coarse olivine, smaller opx and minor cpx; the content and size of olivine gradually decrease as those of opx increase toward the centre of the section where garnet and spinel appear and the cpx becomes abundant; the other side of the section is made up of very large pyroxenes and garnet, both partially replaced with cpx. The sample is believed to have formed by intrusion of a Ca-Al-rich silicate melt, its reaction with host harzburgite and textural equilibration. (b) Olivine-rich domain in peridotite Obn 12-13 similar to the refractory peridotite hosting the vein in Obn 11-13 to its left. (c) Gar-Spl xenolith Obn 21-13 with modal composition transitional between lherzolite and olivine websterite, like in the lower middle part of the Obn 11-13 section to its left. The modally homogeneous Ca-Al-rich lherzolites and pyroxenites in this study may have formed by a similar process on a larger scale. Replacement of garnet and opx rims by cpx (center) may be due to a late-stage metasomatic event, possibly coeval with carbonate formation in other xenoliths not long before the kimberlite eruption. (d) Fine-grained spinel websterite vein in spinel peridotite Obn 63-13 may have formed by intrusion of a silicate melt without significant reaction with the host shortly before the kimberlite eruption.

4.1.2. Carbonate-bearing aggregates

Four peridotite xenoliths contain carbonates (mainly calcite) in fine-grained pockets (Figs. 2a and 4a). In three samples, subhedral calcite grains are texturally equilibrated with olivine and garnet as mosaic aggregates (Fig. 4c and d), which contain no pyroxenes. Phlogopite occurs in peripheral parts of these pockets, but usually not in direct contact with the calcite. To the best of our knowledge, this is the first find of carbonates texturally equilibrated with silicates in peridotite xenoliths from the Siberian craton.

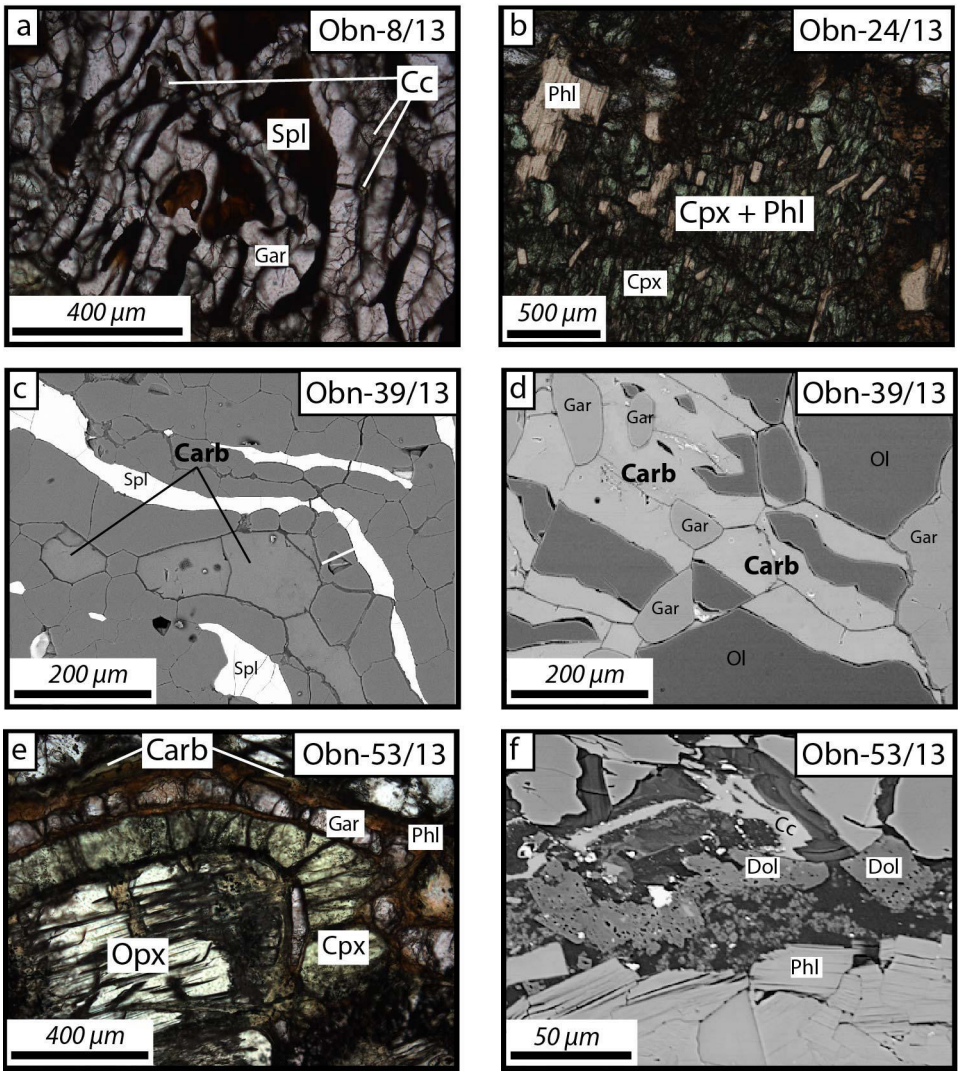

Fig. 4. Photomicrographs in transmitted plane-polarized light (a, b, e), and back-scattered electron (BSE) images (c, d, f) of Obnazhennaya peridotite xenoliths containing carbonate and/or phlogopite (Phl); abbreviations are same as in Fig. 2. (a) Carb-Gar-Ol-Spl pocket similar to those shown in c-d. (b) A fine-grained pocket of Cpx, Phl and Cr-spinel (Cr# 0.94) in Ca-rich, low-Al lherzolite Obn 24-13, likely formed by reaction of carbonate-rich media with the host. (c-d) Carbonate (Mg-Fe-Mn-bearing calcite) texturally equilibrated (straight grain boundaries) with garnet (c) and with garnet and olivine (d) in fine-grained gar-spl-ol pockets containing phl near margins. (e) Opx grain (59 wt.% SiO_2) enveloped by successive layers of cpx (56 wt.% SiO_2), garnet (43 wt.% SiO_2), phl (40 wt.% SiO_2) and carbonates probably formed by reaction of carbonate-bearing, silica-under-saturated liquids with Opx. (f) A close-up of the upper portion of (e) with subhedral dolomite (Dol) and anhedral calcite (Cc) set in a hydrous silicate (antigorite replacing silicate glass?) next to Phl.

Carbonates of proven pre-eruptive, i.e. mantle, origin are extremely rare in cratonic xenoliths, where they can be confused with those related to kimberlite veins and sin- and post-eruption alteration, and have been reported so far only in inclusions in minerals and rare rock types (e.g. Smith, 1987; Lee et al., 2000; Golovin et al., 2017).

Phlogopite of apparent mantle origin, unrelated to kimberlite, has been found only in the four carbonate-bearing samples and in Obn 24-13, which contains fine-grained cpx-phl-spinel pockets (Fig. 4b). In Obn 53-13, carbonates occur in outer parts of reaction zones around opx grains, which consist of (inside-out): opx → cpx → garnet → phl → antigorite; subhedral grains of dolomite and calcite occur in the antigorite, which appears to have replaced fine-grained silicates or glass (Fig. 4e and f, Table S3 of Appendix 1).

4.1.3. Pyroxene-spinel clusters and composite xenoliths

In many peridotites in this study, spinel has peculiar morphology and occurs mainly in clusters with pyroxenes. The most spectacular are vermicular intergrowths of spinel with cpx and/or opx in the form of thin, regularly spaced and similarly oriented curvilinear lamellae inside pyroxenes (Fig. 2b) in samples Obn 12-13 and 22-13. Such spinel-pyroxene clusters, also called symplectites (Field and Haggerty, 1994), are believed to form by breakdown of Al-Cr-rich precursor phases (e.g. Doucet et al., 2012; Casagli et al., 2017).

In pyroxene-rich rocks, spinel forms large irregularly shaped grains located at olivine or pyroxene grain boundaries or intergrown with pyroxenes, which is typical of protogranular microstructure (Mercier and Nicolas, 1975) common in off-craton lherzolite xenoliths.

Some xenoliths show modal variations on mm-cm scale due to irregular distribution of minerals and of spinel-pyroxene or garnet-spinel clusters (Fig. 2) in rocks that appear to be modally homogeneous on hand specimen scale. A few other samples, by contrast, consist of distinct rock types. Such composite xenoliths are grouped in two types. The first type comprises three samples cut by fine-grained websterite veins. Two of them are fine-grained spinel lherzolite (Obn 63-13) and wehrlite (Obn 68-13) with spinel websterite veins ~1 cm thick with gradational contacts (Fig. 3d and Appendix 2). Sample Obn 58-13 is a coarse peridotite containing a thicker (≥5 cm) vein with layering roughly parallel to its contact and variable proportions of pyroxenes, spinel as well as interstitial plagioclase (Appendix 2).

The other type of composite xenoliths is represented by coarse-grained Obn 11-13 that shows modal gradation from olivine-rich peridotite to olivine websterite then to olivine-free spinel-garnet websterite over a distance of ~7 cm (Fig. 3a; Appendix 2).

4.2. Major element compositions and P-T estimates

4.2.1. Major elements in bulk rocks

Whole-rock compositions determined by XRF (on ignited powders) as well as loss-on-ignition (LOI) data are given in Table S2 of Appendix 1 (and Table 1 for Al, Ca, Cr and Mg#) and illustrated in Fig. 5. The LOI range from 0.6 to 8.1 wt.% (mainly 2–5%), as is common for xenoliths in kimberlites, in line with alteration degrees from thin section observations.

In terms of major element compositions, the peridotites are divided into four groups corresponding to those identified in Section 4.1 from petrographic and modal data (Table 1). (1) The four "low-Ca-Al peridotites" have low contents of both Al_2O_3 (≤0.9 wt.%) and CaO (≤0.7 wt.%). (2–3) The eleven "Ca-rich peridotites" contain 1.4–3.2 wt.% CaO at low to moderate Al_2O_3 (0.4–1.9 wt.%), with the highest CaO in the subgroup of five "carbonate-phl-beari ng" samples. Remarkably, seven Ca-rich samples have CaO/Al_2O_3 >2, which is unusual for mantle peridotites in Siberia (Ionov et al., 2015a) and elsewhere (Fig. 5b). (4) The five "Ca-Al-rich lherzolites" contain 2.7–8.0 wt.% Al_2O_3 and 3.2–5.5 wt.% CaO, two other samples in this group are high-Mg# (0.91–0.92) pyroxenites.

The majority of the samples (15 out of 22) show a narrow range of whole-rock Mg# ($Mg\#_{WR}$), from 0.915 to 0.920, in spite of a broad range of CaO and Al_2O_3. Moreover, the highest $Mg\#_{WR}$ of 0.924 among our samples has a Ca-Al-rich lherzolite Obn 6-13 (Table 1). By contrast, harzburgite Obn 60-13 from the low-Ca-Al group has a very low $Mg\#_{WR}$ of 0.888. Most of the xenoliths have higher NiO, and some have lower SiO_2, than common cratonic and off-craton peridotites (Fig. 5c and f); eight samples have very high Cr_2O_3 (0.9–1.4 wt.%; Fig. 5e) as well as high modal spinel or garnet. To sum up, the Obnazhennaya suite shows unusually broad and incoherent variations of major and minor elements and Mg#.

4.2.2. Major elements in minerals

Average mineral compositions are given in Table S3 of Appendix 1; average $Mg\#_{Ol}$ [Mg# in olivine] and $Cr\#_{Sp}$ [molar Cr/(Cr + Al) in spinel] are also listed in Table 1. The Mg# of olivine (major host of Mg and Fe in peridotites) and $Mg\#_{WR}$ show similar values and a good linear correlation (Fig. 6b) except for garnet-rich rocks where $Mg\#_{Ol}$ is much higher than $Mg\#_{WR}$, with the difference ($Mg\#_{Ol} - Mg\#_{WR}$) proportional to modal garnet (Fig. 6c). These relations are imposed by Mg# balance in bulk rocks: because Mg# in garnet is lower than in coexisting olivine (similar FeO at much lower MgO), it is compensated by higher $Mg\#_{Ol}$. This implies that the use of $Mg\#_{Ol}$ as 'depletion' index for garnet-bearing xenoliths in the absence of WR analyses (e.g. Pernet-Fisher et al., 2015) is flawed, e.g. sample Obn 21-13 with $Mg\#_{WR} = 0.900$ has a high $Mg\#_{Ol}$ of 0.922 because it contains 30% garnet with low $Mg\#_{Gar}$ (0.811).

Howarth et al. (2014) reported a $Mg\#_{Ol}$ range of 0.916 to 0.930 for six Obnazhennaya lherzolites, with five $Mg\#_{Ol}$ ≥0.925 and an average of 0.925. By contrast, the average $Mg\#_{Ol}$ for 20 peridotites in this study is 0.916, and no $Mg\#_{Ol}$ ≥0.924. Similarly, the $Mg\#_{Opx}$ in this study are systematically lower (0.91–0.93 vs. 0.91–0.95). We consider that our $Mg\#_{Ol}$ are correct because they are consistent with $Mg\#_{WR}$ obtained by XRF for garnet-free and low-garnet xenoliths (Fig. 6b); the higher $Mg\#_{Ol}$ and $Mg\#_{Opx}$ in Howarth et al. (2014) may be due to biased sampling of garnet-rich rocks and/or analytical problems.

The garnets show a narrow chemical range, with 1.8–2.9 wt.% Cr_2O_3, 3.9–5.5 wt.% CaO and low TiO_2 (≤0.1 wt.%). The Cr_2O_3 contents in particular are generally lower than in garnets in peridotites from Udachnaya and most other cratonic suites (Doucet et al., 2013; Pearson and Wittig, 2014). $Cr\#_{Sp}$ ranges from 0.14 to 0.63, with an outlier of 0.94 in cpx-phl-spinel pockets in Obn 24-13; it shows no correlation with $Mg\#_{Ol}$ (Fig. 6a), but a good correlation (hence chemical equilibration) with $Cr\#_{Cpx}$ for nearly all samples (Fig. 6f).

The carbonate-phl-bearing pockets contain Mg-Fe-Mn bearing calcite with Mg# 0.75–0.84, sample Obn 53-13 also has dolomite with Mg# of 0.97 (Fig. 3f). The phlogopite has 7.9 to 10.9 wt.% K_2O, 0.1–3.5 wt.% TiO_2 and Mg# = 0.88–0.94 (Table S3 of Appendix 1). Plagioclase coexisting with spinel in pyroxenite vein Obn 58-13 is K-free $An_{80}Ab_{20}$.

4.2.3. P-T estimates

Temperature estimates for mantle rocks are mainly based on Ca contents in coexisting pyroxenes. We use here the Ca-opx method of Brey and Köhler (1990) modified by Nimis and Grütter (2010) because the opx in our peridotites has low Na_2O (0.02–0.09 wt.%, mainly 0.02–0.05 wt.%) whereas the cpx has a broad Na_2O range (0.5–2.3 wt.%; Fig. 6e), which may affect T estimates in cpx-based methods due to Na-Ca substitution. A plot of CaO vs. Cr_2O_3 in the

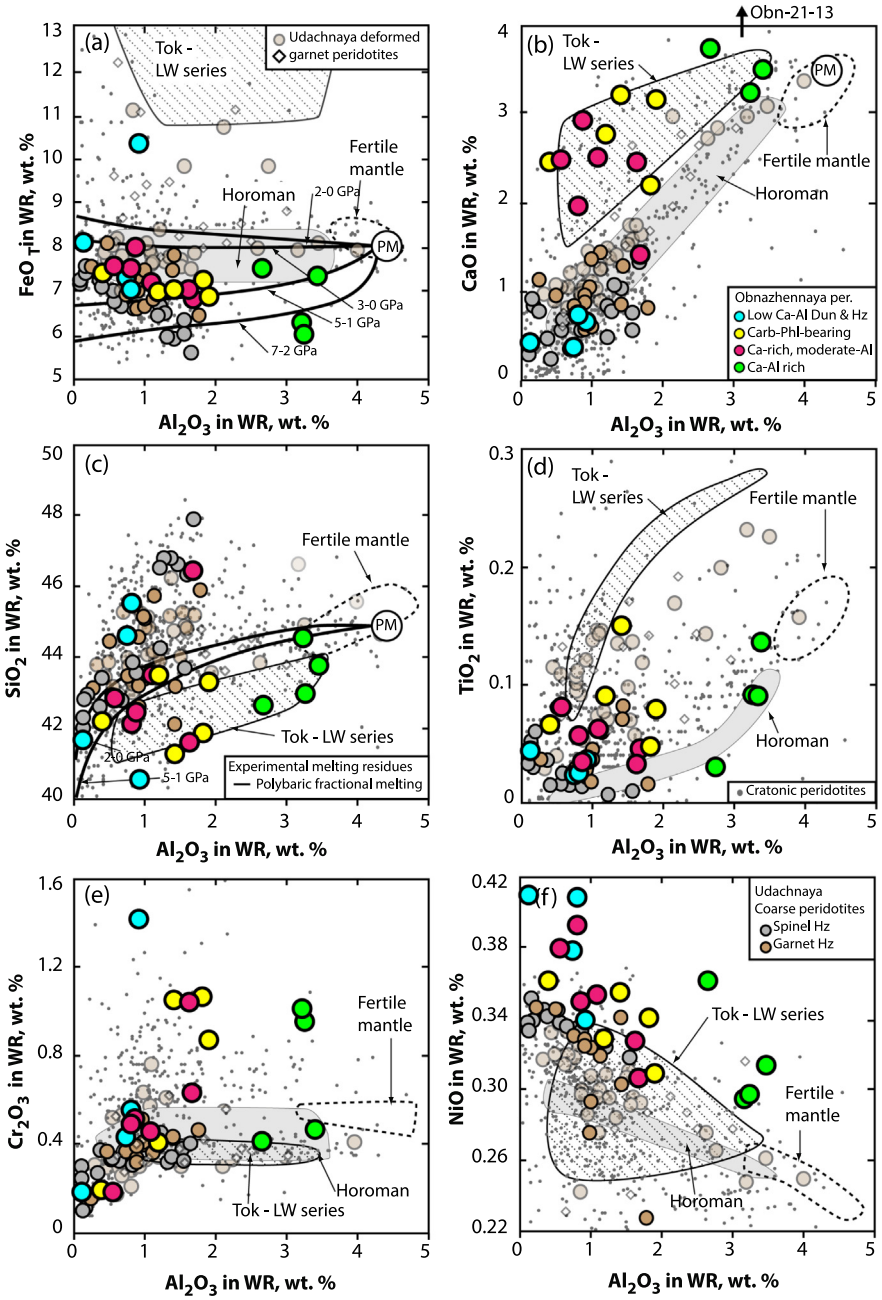

Fig. 5. Co-variation plots of major and minor oxides vs. Al_2O_3 (wt.%) in whole-rock (WR) Obnazhennaya peridotite xenoliths in this study (large circles with thick borders): blue, low-Al-Ca (≤0.9 wt.% CaO and Al_2O_3); yellow, carbonate- and/or Phl-bearing, Ca-rich (1.4–3.2 wt.% CaO) with moderate Al (≤1.9 wt.% Al_2O_3); pink, other Ca-rich peridotites with moderate Al; green, Ca-Al-rich rocks (Obn 21-13 with ~8 wt. % Al_2O_3 is beyond the scale); thick black lines in (a) and (c) are experimental melt residues of polybaric fractional melting (Herzberg, 2004). Also shown are: coarse peridotite xenoliths from the Udachnaya kimberlite in the central Siberian craton (small circles with black borders) after Ionov et al. (2010) and Doucet et al. (2012, 2013), deformed Udachnaya peridotites (small circles with grey borders) after Ionov et al. (2017) and Agashev et al. (2013), primitive mantle (PM) after McDonough and Sun (1995), as well as the fields of fertile off-craton garnet and spinel peridotite xenoliths from Vitim and Tariat in central Asia (fine dashed contours (Ionov et al., 2005a; Ionov and Hofmann, 2007)), Horoman massif peridotites (Takazawa et al., 2000) and the lherzolite-wehrlite (LW) series xenoliths from Tok at the SE margin of the Siberian craton (Ionov et al., 2005b). The majority of the Obnazhennaya peridotites have much higher CaO and NiO than coarse and deformed Udachnaya peridotites, and somewhat higher Al_2O_3 than coarse Udachnaya peridotites. The compositions of Ca-Al-rich Obnazhennaya peridotites are also distinct from those of fertile off-craton lherzolites, and of the Horoman peridotites (residues of melt extraction at low pressures), but show Ca enrichments similar to those in the LW-series peridotites from Tok re-worked by carbonate-bearing basaltic melts.

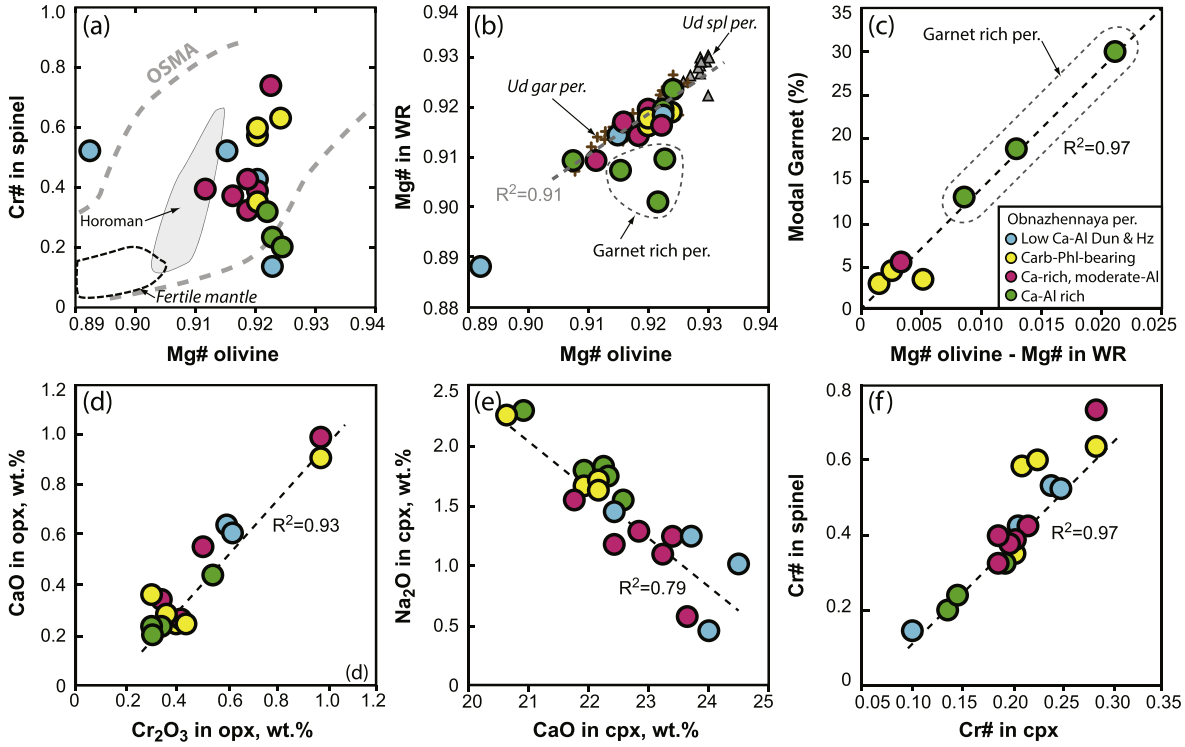

Fig. 6. Plots of major oxides, Mg# $[Mg/(Mg + Fe)_{at}]$ and Cr# $[Cr/(Cr + Al)_{at}]$ in minerals of the Obnazhennaya xenoliths in this study: (a) $Cr\#_{Spl}$ is not correlated with $Mg\#_{Ol}$ and cannot be used as a melt extraction index; (b) $Mg\#_{Ol}$ in garnet-free and low-garnet Obnazhennaya xenoliths shows a good correlation with $Mg\#_{WR}$, like for Udachnaya peridotites (Doucet et al., 2012, 2013), demonstrating consistency of the XRF and EPMA data; (c) differences between $Mg\#_{Ol}$ and $Mg\#_{WR}$ are proportional to the modal garnet, which has much lower Mg# than coexisting olivine; (d) temperature-related co-variation of CaO and Cr_2O_3 (wt.%) in orthopyroxene; (e) high Na and Na-Ca co-variation in clinopyroxenes emphasize the importance of Na-corrections for T estimates; (f) co-variation of Cr# in spinel and clinopyroxene suggesting their chemical equilibration in the majority of the samples.

opx (Fig. 6d) defines a linear correlation and outlines three groups. The opx in two samples with vermicular opx-cpx-spinel clusters has the highest CaO (0.92–0.99 wt.%), four opx have 0.55–0.65 wt.% CaO while all other opx are very low in CaO (0.22–0.36 wt.%). These values yield the T ranges of 1027–1047 °C, 891–933 °C and 668–784 °C using P estimates after Nickel and Green (1985) for garnet-bearing samples, and assuming P = 1.5 GPa for spinel peridotites (Table 1). It is hard to assess if the very low T values for the majority of the samples are robust because they are based on extrapolation of experiments done at ≥900 °C, and because Ca-Mg diffusion becomes sluggish at low T's, which may lead to disequilibrium between the pyroxenes.

The P-T estimates for garnet-bearing samples in this study are shown in Fig. 7 together with those calculated from published EPMA (Taylor et al., 2003; Howarth et al., 2014). Our samples show a P range of 1.6–2.8 GPa (Table 1) and plot on the model geotherms of 40 to >50 mW/m^2, similar to values obtained from literature data. Thus, our results confirm that the Obnazhennaya xenoliths define a much lower P-T range than coarse garnet peridotites from the center of the Siberian craton (~3–7 GPa, 720–1300 °C) (e.g. Goncharov et al., 2012; Doucet et al., 2013) indicating a thin lithosphere with the base at ≤100 km.

A much greater lithospheric thickness of 150 km was inferred for the Kuoika field by Griffin et al. (1999) using

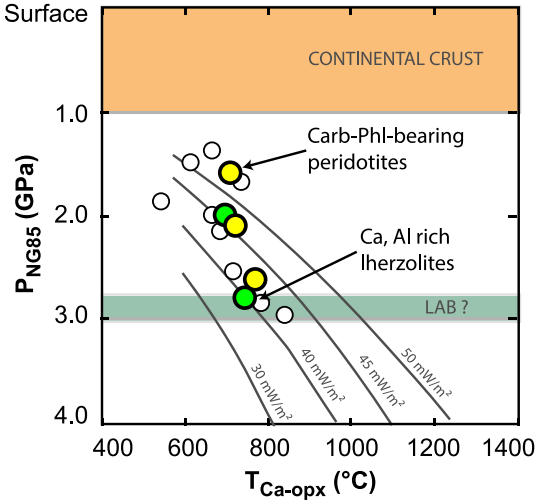

Fig. 7. A plot of P-T estimates after Nickel and Green (1985) and Brey and Köhler (1990) modified by Nimis and Grütter (2010) for garnet-bearing Obnazhennaya xenoliths in this study (large filled symbols) and those calculated from published EPMA (small empty circles, see text for references). The low P range suggests a thin mantle lithosphere with the lithosphere-asthenosphere boundary (LAB) an ≤100 km; the P-T estimates plot on model equilibrium heat flow estimates from 40 to >50 mW/m^2 possibly indicating intra-lithospheric heating by mantle magmatism.

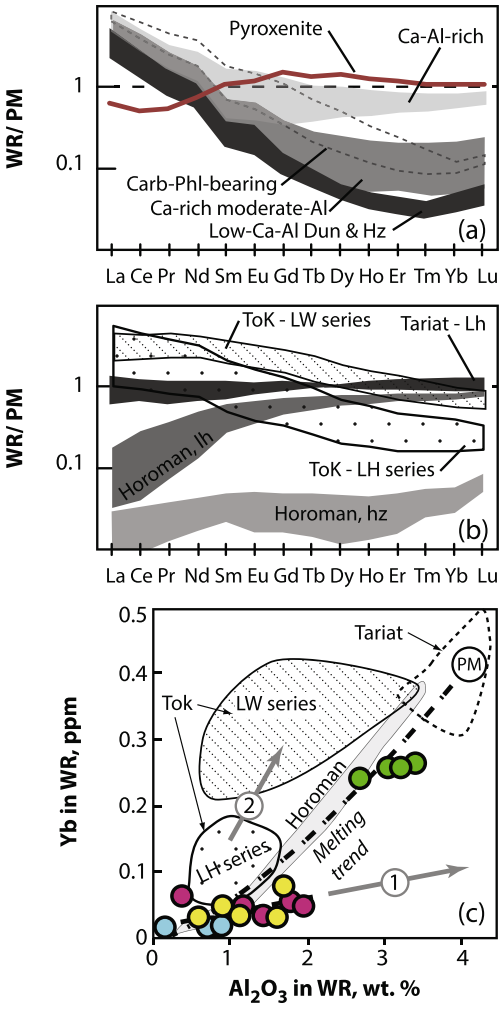

Fig. 8. (a) Primitive mantle-normalized (McDonough and Sun, 1995) REE patterns in whole-rock (WR) Obnazhennaya xenoliths in this study. Fields in shades of grey outline patterns for main peridotite groups, dotted line contours carbonate-bearing peridotites. Red line is for websterite vein Obn 58-13, whose pattern with high heavy REE (HREE) and low light REE is distinct from those of the peridotites. (b) Fields for REE patterns in fertile, near-primitive lherzolite xenoliths from Tariat in Mongolia (Press et al., 1986; Ionov et al., 1997), lherzolites and harzburgites from the Horoman massif (Takazawa et al., 2000) representing melt-depleted, unmetasomatized mantle, and for lherzolite-harzburgite (LH, dotted) and melt-reacted lherzolite-wehrlite (LW, hatched) series xenoliths from Tok in the SE Siberian craton (Ionov et al., 2006a). The REE patterns in the Obnazhennaya and Tok melt-reacted peridotites are distinct from those in moderately melt-depleted or fertile lherzolites (Horoman, Tariat). (c) A plot of Yb vs. Al_2O_3 in WR Obnazhennaya xenoliths; thick dashed line shows melting residues of PM calculated as in Takazawa et al. (2000), abbreviations as in (b), symbols are as in Figs. 5 and 6. The Ca-rich peridotites with low to moderate Al are low in Yb (and other HREE) and define a particular *trend (1)*, probably due to equilibration with low-HREE carbonatite or carbonate-rich silicate melts (Dasgupta et al., 2009), distinct from *trend (2)* for the melting residues and the LH-LW Tok series formed by reaction of residues with basaltic melts. (For interpretation of the references to colour in this figure legend, the reader is referred to the web version of this article.)

garnets from kimberlites. The validity of their method, however, is uncertain because the garnet concentrates may not be representative of common lithospheric rocks, but rather linked to proto-kimberlite activity (e.g. Carlson et al., 2005). Furthermore, it uses a P-T method with questionable accuracy, whose results also contradict the distribution of T's and rock types established by studies of Udachnaya xenoliths (Doucet et al., 2013).

4.3. Whole-rock and mineral trace element compositions

Trace element compositions of bulk rocks and minerals, together with the patterns for REE and REE+Zr+Sr normalized to primitive mantle (PM) for different xenolith groups, are provided in Tables S4 and S5 of Appendix 1.

Bulk-rock REE patterns are shown in Fig. 8a. All the peridotites are enriched in the light (L) relative to medium (M) and heavy (H) REE, but the main peridotite groups differ in the HREE levels, which are the lowest in low-Ca-Al dunites and harzburgites, and the highest in the Ca-Al-rich lherzolites. The plot reveals a 2- to 4-fold gap in HREE between the Ca-Al-rich and other peridotites while the differences in Al_2O_3 contents are much smaller (1.5-fold). This gap is also evident on a plot of Yb vs. Al_2O_3 (Fig. 8c) where the peridotites with low to moderate Al define a linear trend pointing away from the Ca-Al-rich rocks and fertile mantle. The REE pattern of coarse garnet pyroxenite O-1080 is LREE-enriched like those of the peridotites, but the fine-grained spinel-pl websterite vein Obn 58-13 shows a LREE-depleted pattern distinct from those for all other samples in this study (Fig. 8a).

Extended WR element patterns usually have negative Zr-Hf and positive Sr anomalies (Table S4 of Appendix 1). The contents of V and Sc are positively correlated with Al, but no other moderately (e.g. Yb, see above) or highly incompatible elements define regular correlations with Al, unlike in peridotite xenoliths from Udachnaya (e.g. Ionov et al., 2017).

The cpx with vermicular spinel inclusions have peculiar REE patterns, with a steep decline from HREE to MREE (Figs. 2b and 9b and c), similar to those in garnets (Fig. 10c and d), but distinct from those for other cpx that are nearly flat or LREE-enriched. The cpx from garnet-bearing rocks are LREE-rich, usually with a hump at Nd (Fig. 10a and b). Garnets from Ca-Al-rich rocks have the highest HREE-MREE and are equilibrated with coexisting cpx (Fig. 10d and f). By contrast, garnets from carbonate-bearing peridotites have lower and more variable HREE and are usually out of equilibrium with cpx from the same samples (Fig. 10c and e).

5. DISCUSSION

The Obnazhennaya samples represent a most unusual cratonic mantle xenolith suite. Re-Os isotope data indicate that its lithospheric sources formed by melt extraction in the Archean to Paleoproterozoic (Ionov et al., 2015a), as is common for cratons. Yet, unlike xenoliths from the Udachnaya and other kimberlites in Siberia, or the majority of those from other cratons, the Obnazhennaya suites in

this and earlier studies have no sheared peridotites, show low P-T values, and have many rocks rich in pyroxenes and garnet rather than refractory harzburgites. We attribute these features to widespread reworking of initial mantle lithosphere, and use the new data in this study to explore the mechanisms and implications of this process.

5.1. Any chemically pristine remnants of initial mantle lithosphere?

5.1.1. Low-Ca-Al dunites and harzburgites

Coarse cratonic peridotites believed to be residues of high-degree melting typically have high $Mg\#_{WR}$ ≥0.92 and low Al and Ca (Boyd, 1989; Boyd et al., 1997; Herzberg et al., 2010). In particular, a large number of spinel and garnet peridotite xenoliths from Udachnaya, the best studied suite of mantle rocks on the Siberian craton, were earlier interpreted as nearly pristine, in terms of modal and major oxide compositions, residues of ~40% polybaric melt extraction (Doucet et al., 2012, 2013). Likely candidates to be residues of high-degree melting among the samples in this study are the low-Ca-Al dunites and harzburgites. However, modal and chemical data on these samples suggest strong effects of melt metasomatism, which conceals their origin (Herzberg and Rudnick, 2012).

Dunites are not likely to be melting residues because opx disappears at very high melting degrees of ≥50% (e.g. Walter, 2003), and are believed to be melt channel materials formed by reaction of peridotites with migrating melts (Kelemen, 1990). Experimental and natural data indicate that vein peridotites show broader ranges of modal and chemical compositions than high-degree melting residues, depending on melt composition and position in channels (Takahashi et al., 1992; Morgan and Liang, 2005; Tursack and Liang, 2012; Mitchell and Grove, 2016). In this regard, a melt-reaction origin for opx-free dunites Obn 59-13 and 60-13 is supported by their relatively high FeO (Fig. 5a) and low Mg# (0.888 and 0.916) as well as considerable scatter in the contents of Cr_2O_3 (0.18 and 1.41 wt.% compared to 0.3–0.5 wt.% in residual peridotites; Fig. 5e), NiO (0.34 vs. 0.41 wt.%) and modal spinel.

The other two samples in this group, by contrast, have high modal opx (24–27%) and are enriched in SiO_2 relative to experimental melting residues (Fig. 5c), which may be due to melt-rock reaction as well (Kelemen et al., 1992). Like the dunites, they have higher FeO (Fig. 5a) and lower Mg# <0.92 than spinel harzburgites with similar Al and Ca contents from Udachnaya and typical refractory cratonic peridotites worldwide (Pearson et al., 2014).

Post-melting modifications of these four samples are supported by their perturbed PGE abundances (Ionov et al., 2015a), e.g. Os is low in three out of four xenoliths (0.6–2.2 ppb compared to 2.4–9 ppb in other Obnazhennaya peridotites), but extremely high (35 ppb) in Obn 59-13 (Table S6 of Appendix 1), both likely due to melt migration. Ionov et al. (2015a) argued that Re-Os model ages in this group may be compromised, e.g. three samples have the lowest T_{RD} values among the Obnazhennaya peridotites with low to moderate Al (Table 1).

5.1.2. Harzburgites and lherzolites with low to moderate Al

Eleven xenoliths have fairly low (≤1.9 wt.%) Al_2O_3 (considered to be the most robust melt extraction index) and could be melting residues. Yet all show petrographic and/or chemical features that cannot be explained by melt extraction alone: late-stage cpx or carbonate, broadly variable and often anomalously high CaO (up to 3.2 wt.%; Fig. 5b), Ca/Al ratios (up to 8) and Cr_2O_3 (up to 1.1 wt.%; Fig. 5e). Overall, these data suggest chemical and modal metasomatism via interaction of what were initially refractory melt residues with migrating melts, but some, like higher NiO than in residual peridotites from Udachnaya and other cratonic suites (Fig. 5f), are puzzling.

Because the Obnazhennaya peridotites are not pristine melting residues, the chemical data do not allow to constrain reliably the nature and conditions of the events that formed initial mantle lithosphere 2–3 Gy ago (Ionov et al., 2015a). In particular, post-melting processes affected the Fe and Al contents and Mg#, essential parameters to establish the degrees and pressure of melting (Walter, 1999; Herzberg, 2004). As a result, the generally higher FeO in the peridotites with low to moderate Al_2O_3 in this study than in residual peridotites from Udachnaya (Fig. 5a), which may suggest melting at lower pressures, could alternatively be due to post-melting Fe-enrichments.

5.2. Metasomatism by carbonate-rich melts

5.2.1. Formation of carbonates

Metasomatism by carbonatite or carbonate-rich silicate melts is often evoked for mantle rocks, e.g. based on high Ca/Al, La/Yb and low opx (Yaxley et al., 1991; Hauri et al., 1993; Rudnick et al., 1993; Wiechert et al., 1997), but finds of mantle-derived carbonates in peridotite xenoliths are very rare (Ionov et al., 1993; Lee et al., 2000), in particular on cratons. Their rarity is attributed to pervasive reaction of carbonate-rich melts with opx (which has the highest SiO_2 in the peridotites) to form cpx and olivine (e.g. Dalton and Wood, 1993). In most cases, the carbonates are found as inclusions in minerals (Yaxley et al., 1998) or as interstitial calcite aggregates, texturally and chemically unequilibrated with the host, and interpreted as cumulates from ephemeral carbonatite liquids (Ionov, 1998; Lee et al., 2000). By contrast, carbonates equilibrated with host peridotites are exceptional (Ionov et al., 1996). This is why the discovery of mosaic aggregates of calcite, garnet and olivine in three samples in this study (Figs. 2a and 4) is of particular importance, not only as the first find of granular carbonates in peridotite xenoliths from the Siberian craton, but also as arguably the first case of texturally equilibrated carbonates (Fig. 4c and d) in cratonic peridotites.

This shows that the metasomatism may affect cratonic mantle not only by equilibration of existing silicate minerals with carbonate-rich media or formation of metasomatic silicates like amphibole and cpx (Green and Wallace, 1988), but also by precipitation of carbonates. The peridotites in this study contain calcite whereas experimental work (e.g. Dalton and Wood, 1993) suggests that carbonatite melts at 1.5–3 GPa are dolomitic to magnesiocalcitic. The

mineralogy of the carbonate-bearing pockets (calcite equilibrated with olivine and garnet) suggests that they may have formed via reaction of dolomitic melt with pyroxenes to yield olivine and calcite (e.g. Bussweiler et al., 2016). Also, because garnet in these xenoliths occurs mainly, if not exclusively, in the metasomatic pockets (Fig. 2a), and because calcite is not found in direct contact with spinel (Fig. 4c), the garnet could form in a de-carbonation reaction as well: dolomitic melt + cpx + spl ± opx → olivine + garnet + calcite + CO_2.

The carbonates may be equilibrated only with minerals (olivine, garnet ± phl) within the metasomatic pockets, but probably not with coarse pyroxenes beyond the pockets in the same xenoliths, e.g. Obn 08-13 (Fig. 2a). This is consistent with disequilibrium REE distribution in these rocks between the garnet and cpx (Fig. 9e). Overall, the carbonates may be transient phases destined to react out with time either via chemical exchange with opx over greater distances in rocks or due to changing P-T-fO_2 conditions (Brey et al., 1983; Dalton and Wood, 1993; Foley, 2008). Yet, their chemical components like Ca, Sr and LREE remain in the rocks hosted by silicates, most likely cpx, ultimately formed by reactions with the calcite (e.g. Yaxley et al., 1991; Rudnick et al., 1993; Neumann et al., 2002). The low P_2O_5 contents (≤0.01 wt.%) in our samples suggest they contain no phosphates often associated with carbonatite metasomatism (e.g. Ionov et al., 2006a).

5.2.2. Replacement of opx by cpx and garnet

Coatings around opx grains in sample Obn 53-13 (Fig. 4e) are a sequence of minerals with decreasing SiO_2 from opx (59 wt.%) to cpx (56 wt.%), garnet (43 wt.%) and phl (40 wt.%). We interpret this zoning as a result of reaction of opx with silica-undersaturated liquids, likely carbonated silicate melts (Dalton and Presnall, 1998), to reduce modal opx in peridotites and replace it with cpx ± garnet as suggested by experimental work (e.g. Dalton and Wood, 1993; Gervasoni et al., 2017). The replacement of opx by cpx may have affected mainly olivine-rich rocks that are particularly permeable for carbonate-rich liquids (e.g. Hunter and McKenzie, 1989), like Obn 53-13 where many opx grains are rimmed with cpx. Another spectacular example of such a process are fine-grained aggregates of cpx and olivine (± amphibole) replacing opx in Obn 24-13 and 48-13 (Appendix 2).

The nature of carbonates in Obn 53-13 (Fig. 4f) should be assessed with caution because they occur inside post-eruption hydrous minerals and include dolomite that was not found in samples with texturally equilibrated carbonates. It is tempting to attribute the carbonates in Fig. 4f to crystallization of late-stage derivatives of carbonate-bearing melts after reaction with opx. However, they may alternatively be linked to alteration of the xenolith during and after the emplacement of the host kimberlite.

5.2.3. Chemical effects of 'carbonatite' vs. 'silicate' metasomatism

Metasomatism by carbonate-rich media may be the major reason for high Ca and Ca/Al in the Obnazhennaya peridotites with low to moderate Al, including carbonate-free rocks that may have previously contained carbonates that reacted out to form silicates (e.g. Dalton and Wood, 1993; Gervasoni et al., 2017). The Ca-enrichments in these peridotites are greater than those reported for peridotites from Udachnaya and most other cratonic suites (Fig. 5b), and appear to be specific to the mantle beneath Obnazhennaya. The carbonate-bearing peridotites with low to moderate Al have the highest LREE to HREE ratios (Fig. 8a) and contain the cpx with the highest LREE in this study (Figs. 9 and 10).

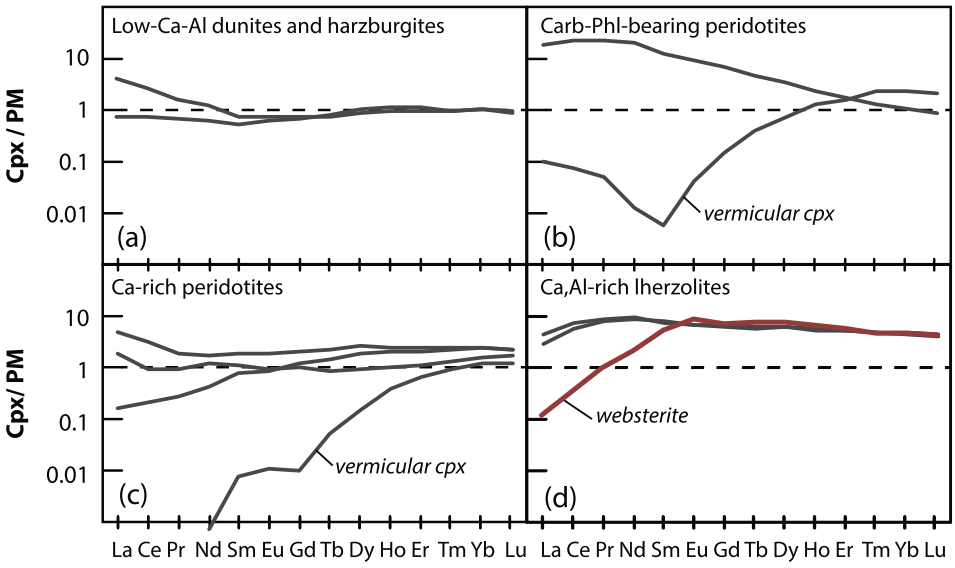

Fig. 9. Primitive mantle-normalized (McDonough and Sun, 1995) REE patterns for cpx in spinel peridotites from Obnazhennaya in this study: (a) low-Ca-Al dunites and harzburgites, (b) carbonate-bearing Ca-rich, moderate-Al, (c) carbonate-free Ca-rich, moderate-Al, (d) Ca-Al-rich peridotites and websterite. REE patterns of vermicular cpx are distinct from those for other peridotites in the same groups because they are garnet breakdown products (see text).

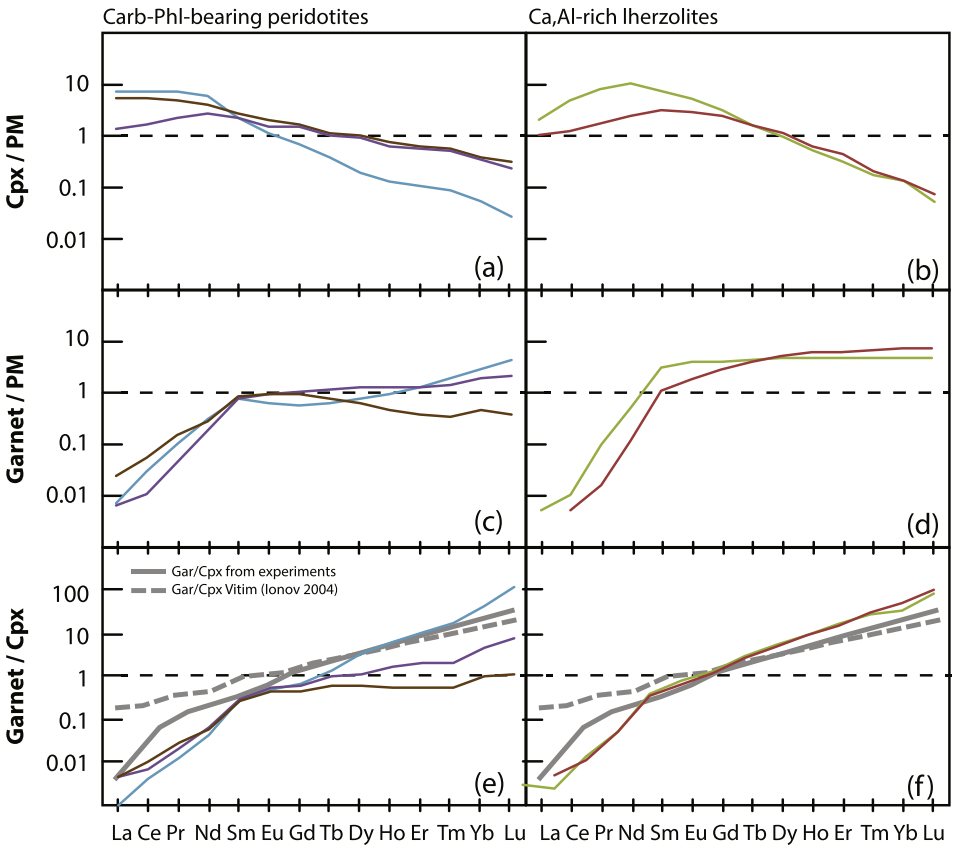

Fig. 10. Primitive mantle-normalized (McDonough and Sun, 1995) REE patterns for cpx (top), garnet (middle) and garnet/cpx ratios (bottom) in garnet peridotites from Obnazhennaya in this study. Left column, carbonate-bearing peridotites with moderate Al; right column, Ca-Al-rich lherzolites. Garnet and cpx in the Ca-Al-rich rocks appear to be in equilibrium with each other (because the garnet/cpx ratios for the REE are similar to those in experiments (e.g. Gaetani et al., 2003) and in equilibrated garnet peridotite xenoliths (Ionov, 2004; Ionov et al., 2005a). The cpx appear to be equilibrated with silicate melts because they have humped MREE-LREE patterns with summits near Nd typical of melt-equilibrated cpx (Ionov et al., 2002 and references therein). Garnet and cpx in many carbonate-bearing rocks are out of equilibrium and differ in metasomatic enrichment degrees.

It is fitting to compare the samples in this study with basalt-hosted peridotites from Tok in the SE Siberian craton (Ionov et al., 2005c; Fig. 1), which like the xenoliths from this study come from the craton's margin and show widespread metasomatism. The Tok xenoliths, in particular those of the lherzolite-wehrlite (LW) series, commonly have high CaO and Ca/Al ratios (Ionov et al., 2005b, 2006a), like many samples in this study. By contrast, the Tok LW xenoliths also show strong enrichments in Fe, Ti (Fig. 5a and d) and HREE (Fig. 8c), which are rare or absent in our Obnazhennaya suite. The combination of high CaO, Ca/Al and LREE/HREE with low to moderate Mg# and Ti and Al in the Obnazhennaya peridotites suggest metasomatism by carbonate-rich melts rather than by the evolved silicate liquids inferred for Tok (Ionov et al., 2006a). In any case, we argue that widespread Ca enrichments and high Ca/Al may be typical for reworked cratonic domains, possibly linked to their position near craton rims, which is what the Obnazhennaya and Tok sites have in common.

Metasomatism by low-Os carbonatite melts (Aulbach et al., 2016) may also explain why the Os-isotope compositions of the initial refractory precursors of the Obnazhennaya peridotites, which yield the highest Re-Os model ages among our samples in spite of high CaO (Table 1), were not reset, but only minimally affected (Ionov et al., 2015a), by comparison with greater effects of reaction with evolved basaltic melts on the LW series Tok xenoliths, whose Re-Os and PGE systematics have been largely reset (Ionov et al., 2006b).

5.3. Ca-Al-rich products of silicate melt metasomatism

The Ca-Al-rich Obnazhennaya peridotites have peculiar modal and chemical compositions. They combine, on one hand, features of refractory melting residues like variable, but usually high, modal olivine, high $Mg\#_{WR}$ (0.900–0.924 including the highest value in this study) and Cr, and on the other hand, high LREE, high modal cpx (up to 22%) and garnet (up to 30%) as well as low opx (5–7% in three samples). These rocks also have high Na_2O (average 0.2 wt.%) and higher Ca/Al than fertile to moderately depleted off-craton lherzolites (and PM) (Fig. 5b). The average contents of Al_2O_3 (4.1 wt.%) and CaO (4.2 wt.%) in the Ca-Al-rich rocks are much higher than in peridotites

with low to moderate Al (1.2 wt.% Al_2O_3, 2.5 wt.% CaO), but average $Mg\#_{WR}$ in the former is only marginally lower (0.912 vs. 0.917) while average $Mg\#_{Ol}$ are almost the same (0.918 vs. 0.919, Section 4.2.2).

We argue that the Ca-Al-rich rocks are 'hybrid', i.e. formed by mingling and reaction of refractory melting residues, from which they inherited high Mg, Cr and Ni, with melts, which added Al, Ca, Na and REE (Fig. 7) (e.g. Rehfeldt et al., 2008). A graphic model for this process can be seen in Fig. 3a–c, which compares the cross-section of composite sample Obn 11-13 with a harzburgite and a websterite xenoliths that represent its initial and final stages. Crystallization of melt in a conduit formed olivine-bearing (Obn 14-13, 21-13) or olivine-free (O-1, Obn 28-13) websterites; the initial or residual melt migrated into wall-rock harzburgite and reacted to form pyroxenes and garnet, whose amounts decrease away from the conduit. A late-stage reaction formed cpx at the expense of opx ± garnet (Fig. 3a and c), which may explain high Ca/Al and low opx in the peridotites.

The nature of the melts is hard to constrain. They must be Mg-rich and low in Ti and alkalis, like near-primitive products of mantle melting, yet enriched in LREE because of high LREE in the Ca-Al-rich rocks (Fig. 8a). It is common to attribute LREE-enrichments in WR xenoliths hosted by kimberlites to contamination by host magma and alteration, but we note that sample Obn 58-13 (see next section) is LREE-depleted, which renders such an argument less relevant. Estimates of melt REE contents using cpx/melt partition coefficients and cpx analyses (Figs. 9 and 10) yield slightly LREE-enriched patterns. Further, these melts can be neither carbonatites (low in Al and HREE) nor Fe-Ti-rich silicate melts (Fig. 5a and d), the latter discerns the Ca-Al-rich peridotites in this study from the LW-series xenoliths from Tok (Figs. 5 and 8) affected by evolved CO_2-rich basaltic melts (Ionov et al., 2005b, 2006a). Gao et al. (2008) argued that Archean lithospheric mantle in North China was hybridized before its ultimate removal by melts derived from foundered lower crustal eclogite.

5.4. Sequence of mantle events in the SE Siberian craton

5.4.1. Lithospheric mantle formation and re-working

Re-Os isotope data on samples in this study (Ionov et al., 2015a) show that the lithospheric mantle beneath Obnazhennaya was formed in two distinct ancient events: the first one near the end of the Archean (~2.8 Ga) and the second in the Paleoproterozoic (~2.0 Ga) (Fig. 11), which added new materials to the existing lithosphere (Ionov et al., 2015b). The magmatic event that produced Re and Ca-Al enrichments in lherzolite Obn 21-13 could be roughly coeval with the Archean melt extraction event (Ionov et al., 2015a). In any case, the Ca-Al-rich rocks must have formed early enough to allow the development of coarse microstructures and cooling to ambient temperatures before the capture by kimberlite magma ~160 My ago.

The ages of multiple enrichment events cannot be established with any available data on Obnazhennaya xenoliths. However, indirect evidence is provided by the age distribution of zircon xenocrysts in kimberlites (Fig. 11) originating from lower crust or metasomatized mantle. The zircons from the Obnazhennaya and other Kuoika field kimberlites include a group with Phanerozoic (200–550 Ma) ages (Kostrovitsky et al., 2016), indicating magmatic episodes at the NE margin of the Siberian craton, possibly linked to metasomatic events documented in this study. By contrast, the Anabar zircons (from the inner craton) show only Archean to Proterozoic ages, in line with two stages of lithosphere formation on the Siberian craton (see Moyen et al., 2017; Paquette et al., 2017 for a review).

We are not aware of any robust evidence on the thickness of the lithosphere beneath Obnazhennaya when its formation was completed ~2.0 Gy ago. If it was thicker initially, the timing and causes of its subsequent thinning

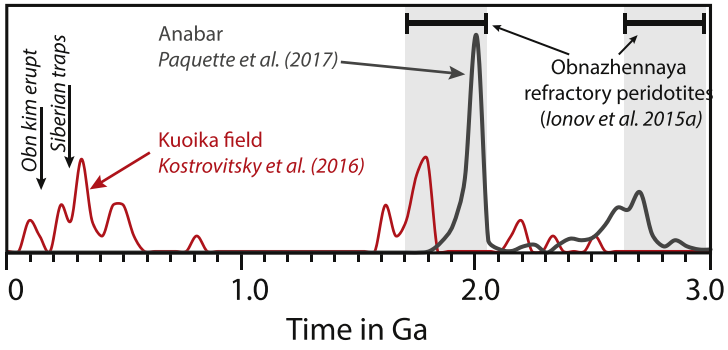

Fig. 11. Age probability plots for zircon xenocrysts (originating from lower crust or metasomatic mantle) in kimberlites from the Kuoika field (red line) (Kostrovitsky et al., 2016) and for detrital zircons from the Anabar shield (grey line) (Paquette et al., 2017). The zircons from the Obnazhennaya and other Kuoika field pipes include a considerable group with Phanerozoic (200–550 Ma) ages, indicating magmatic events in the lithosphere at the NE margin of the Siberian craton. By contrast, the Anabar zircons (inside the craton) show only Archean to Proterozoic ages, corresponding to two stages of lithosphere formation on the Siberian craton shown as horizontal bars (Ionov et al., 2015a,b; Moyen et al., 2017), but no Phanerozoic magmatism. Black vertical arrows mark the eruption ages of the Obnazhennaya kimberlite (160 Ma) and of the Siberian traps (250 Ma). The latter is distinct from the maxima (~300 Ma, 500 Ma) for the Phanerozoic Kuoika zircons providing further evidence against the links between the plume-related trap magmatic event and kimberlitic magmatism (Sun et al., 2014) or mantle metasomatism. (For interpretation of the references to colour in this figure legend, the reader is referred to the web version of this article.)

are hard to constrain. We see no particular reason to attribute the hypothetical lithospheric erosion, nor all or the majority of the metasomatic overprints recorded in Obnazhennaya xenoliths, to the mantle plume responsible for Siberian flood basalt volcanism as advocated by Howarth et al. (2014) and Pernet-Fisher et al. (2015). First, it is highly speculative to infer this from chemical analyses of major minerals in few small samples alone, as done by those authors. Moreover, Obnazhennaya is too far away from the presumed trajectory of the plume to have been affected, and the majority of Phanerozoic alkaline or mafic magmatic events documented by zircon megacrysts in the Obnazhennaya kimberlite are older than the traps while kimberlites from Anabar, much closer to the trap eruption centers, show no Phanerozoic zircons at all (Fig. 11).

5.4.2. Late-stage lithospheric mantle events

Several events recorded in our xenoliths may have taken place shortly before their capture by kimberlite. The vermicular pyroxene-spinel aggregates in Obn 22-13 and 12-13 (Fig. 2b) could not be texturally stable at >1000 °C for a long time. They formed by rapid breakdown of garnet probably in response to a local rise in temperature due to a magmatic event; a drop in pressure is not a viable alternative in mantle lithosphere. Samples not affected by heating remained in the garnet stability field; the usual coexistence of garnet and spinel is due to a broad range of P-T conditions at which both garnet and spinel are stable in the mantle (Ziberna et al., 2013). Another late-stage event was the formation of fine-grained, phl-bearing pockets (Figs. 2a and 4) due to percolation of carbonate-rich melts.

Fine-grained spinel websterite veins in three xenoliths (texturally and chemically distinct from coarse websterites) formed shortly before the kimberlite eruption as well because long residence in the mantle leads to recrystallization to more coarse and texturally equilibrated rocks. The absence of sharp contacts with host peridotites excludes an origin by intrusion of the magma that carried the xenoliths. Chemical data for vein Obn 58-13 rule out any links to kimberlitic or related liquids: it is LREE-depleted, with lower LREE and higher HREE than in any other sample (Fig. 8a); it also contains low-Mg# opx (0.82 vs. 0.91 for olivine in the host peridotite), Cr-poor spinel (Cr# 0.03) and K-free plagioclase (An_{80}). Together with modal and textural layering parallel to vein contacts, this argues for a cumulate origin from a moderately evolved, low-alkali, low-Ti, LREE-depleted silicate melt, possibly akin to MORB. Veins Obn 63-13 and 68-13 may be cumulates from similar, but less evolved liquids.

5.5. Obnazhennaya xenoliths in the light of 'refertilization' models

5.5.1. No typical fertile lherzolites in the metasomatized Obnazhennaya suite

Modification of lithospheric mantle by interaction with fluids or melts has been known for over four decades as "mantle metasomatism". This process is called 'cryptic' if it involves minor chemical changes, mainly in trace elements, or alternatively, 'patent' (Dawson, 1984) or 'modal' if it deposits new phases (Harte, 1983) or affects mineral proportions, and can be further subdivided into 'fluid', 'melt', etc. The concept of 'refertilization' was initially applied to abyssal peridotites, often plagioclase-bearing, injected by liquids similar to those previously extracted from asthenospheric mantle to obtain their melt-depleted protoliths (Elthon, 1992). Later, however, it was extended to include enrichments of incompatible trace elements (e.g. Hellebrand et al., 2002) thus duplicating the notion of "mantle metasomatism" by replacing it with a more vague term, or using both, which is confusing.

A major problem with the concept of 'refertilization' is that it is occasionally invoked to argue, contrary to experimental results and natural observations (e.g. Tursack and Liang, 2012; Wang et al., 2016; Gervasoni et al., 2017), that percolation of metasomatic melts can convert ancient refractory cratonic harzburgites to 'fertile' lherzolites, identical in modal, chemical and isotope compositions to those generally believed to be products of low-degree melt extraction from primitive mantle (Salters and Stracke, 2004). The topic is important because such fertile (capable to produce basaltic magmas) lherzolites are major components of the asthenosphere and are common in off-craton continental lithospheric mantle (CLM), e.g. in central Asia (Ionov et al., 2005a; Ionov and Hofmann, 2007).

Several publications (e.g. Zhang et al., 2008; Tang et al., 2013) evoke 'refertilization' of refractory Archean mantle lithosphere beneath the North China craton in the Phanerozoic as a major process in the formation of the modern fertile to moderately melt-depleted CLM in northern China and elsewhere, contrary to the overwhelming evidence for their origin by melt extraction (e.g. Rudnick et al., 2004). Such an origin is very unlikely, e.g. because it implies that the same liquids as those extracted in the Archean were added to the residues in the same proportions in the Phanerozoic, when such liquids do not exist or are extremely rare (Herzberg and Rudnick, 2012). This hypothesis can be further tested using the data on the xenoliths in this paper, which document a natural suite of rocks formed by melt metasomatism, i.e. 'refertilization', of refractory Archean materials.

As repeatedly noted in preceding sections, none of our samples has modal, chemical or Os-isotope compositions similar to those of primitive or slightly to moderately melt-depleted mantle. The same is valid for an extensive suite of melt-metasomatized peridotite xenoliths hosted by basalts at Tok in the SE Siberian craton. Both xenolith suites define metasomatic trends distinct in modal, major and trace element abundances from those of natural variably melt-depleted peridotite series (e.g. Horoman, Hannuoba, Tariat, Vitim, Figs. 5 and 8) or model melting residues of primitive mantle. Thus, our data, together with experimental evidence examined in Sections 5.1-5.3 argue against refertilization of Archean lithosphere as a major process in the origin of off-craton CLM in central and eastern Asia or elsewhere. We note however that mingling and reaction of refractory mantle with migrating melts may be important locally, e.g. in the origin of peridotite-pyroxenite series in orogenic massifs (Bodinier et al., 2008), and that 'auto-refertilization' during adiabatic

melting may contribute to modal and major oxide variations in mantle lithosphere (Rudnick and Walker, 2009).

5.5.2. Os isotope and PGE considerations

Pristine refractory cratonic peridotites normally have $^{187}Os/^{188}Os$ ratios of 0.105–0.115 resulting in T_{RD} model ages of 3–2 Ga; for off-craton peridotites the range is 0.115–0.130 (T_{RD} 2–0 Ga) including 0.125–0.130 for fertile mantle (e.g. Meisel et al., 2001; Pearson et al., 2004; Carlson, 2005). These differences in Os isotope composition is a major stumbling block for models of 'refertilization' of ancient refractory peridotites by migrating melts to produce off-craton CLM. Because Os abundances in Phanerozoic mantle-derived melts are orders of magnitude lower than in the residues, the melts cannot raise $^{187}Os/^{188}Os$ ratios in large volumes of ancient refractory peridotites by host-melt equilibration at plausible melt/rock ratios. Moreover, at high melt/rock ratios, melts dissolve primary sulfides, producing discordant, low-Os dunites rather than fertile lherzolites (e.g. Rudnick and Walker, 2009). Calls for widespread refertilization of Archean mantle lithosphere (e.g. Zhang et al., 2008; Tang et al., 2013) either ignore this topic or invoke dubious mechanisms like mixing of refractory rocks with asthenospheric material, or major addition of sulfides with radiogenic Os, in spite of evidence that the Re-Os systematics appear to be unperturbed in xenoliths from North China with multiple generations of sulfides (e.g. Gao et al., 2002).

Sulfides have not been found by petrographic inspection of our xenoliths. Archean T_{RD} ages were obtained on our xenoliths with up to 1.8 wt.% Al_2O_3 and 2.5 CaO wt.%, and Paleoproterozoic T_{RD} on xenoliths with up to 3.2 wt.% Al_2O_3 and 3.2–4.9 wt.% CaO (Ionov et al., 2015a), implying that significant enrichments in the 'basaltic' major oxides may not be mirrored by changes in Os isotope ratios.

Chu et al. (2009) argued that Os isotope data for mantle xenoliths from the North China craton are consistent with thinning of its eastern part as a result of foundering of the deep crust and lithospheric mantle, but are inconsistent with stretching or refertilization models, as remnants of Archean mantle are expected to be present in these scenarios. The findings of this study agree with this inference because the Obnazhennaya suite, a natural example of reworking of cratonic lithosphere, includes peridotites with Archean Os ages as well as chemical traces of the initial lithosphere as low Al and high Mg# in strongly modified rocks.

6. CONCLUSIONS

(1) The Obnazhennaya kimberlite in the NE Siberian craton hosts a most unusual cratonic xenolith suite, with common rocks rich in pyroxenes and garnet, no sheared peridotites and low P-T values from a very thin mantle lithosphere (≤100 km).
(2) The peridotites with low to moderate Al contents and Archean to Paleoproterozoic Os isotope ages show widespread reworking of initial mantle lithosphere by a range of liquids from carbonate-rich, silica-undersaturated to MORB-like.
(3) Metasomatic pockets of calcite texturally equilibrated with garnet and olivine, previously unknown in cratonic peridotites, suggest that carbonatite metasomatism may produce enrichments in the mantle not only by equilibration of existing or the formation of new silicate minerals with carbonate-rich melts, but also directly by precipitation of carbonates.
(4) Pervasive inter-granular percolation of highly mobile and reactive carbonate-rich liquids may reduce the strength of the mantle lithosphere leading the way for reworking by silicate melts particularly effective at craton margins.
(5) Specific modal, chemical and Os-isotope features of the melt-reacted Obnazhennaya xenoliths (high Ca/Al, uncorrelated Mg# and Al, variable Cr, low $^{187}Os/^{188}Os$, continuous and broad modal range) are distinct from those of fertile to moderately melt-depleted lherzolites in off-craton mantle. They argue against the concept of 'refertilization' of cratonic harzburgites by mantle-derived melts as a major mechanism to form fertile lherzolites in continental lithospheric mantle.

ACKNOWLEDGEMENTS

DAI acknowledges the Chinese Academy of Sciences President's International Fellowship Initiative (PIFI) for Visiting Scientists in 2017 taken up at GIG (Guangzhou) and thanks B. Moine, C. Guilbaud and J. Chevet for assistance with sample processing at Jean Monnet University (St Etienne, France). Financial support was also provided to DAI by the French CNRS via INSU-PNP grants for mantle studies in 2013-17, and to LSD by the Belgian F.R.S-FNRS "mandat Chargé de Recherche" n°1.B.102.14F. AVG was supported by Russian state assignment project n° 0330-2016-0006. We would like to thank Paolo Nimis for advice on P-T estimates, Fernanda Gervasoni and two anonymous reviewers for extensive comments that helped us to improve the manuscript, and Mark Rehkämper for advice and efficient editorial handling.

APPENDIX A. SUPPLEMENTARY MATERIAL

Supplementary data associated with this article can be found, in the online version, at https://doi.org/10.1016/j.gca.2017.12.028. These data include Google maps of the most important areas described in this article.

REFERENCES

Agashev A. M., Ionov D. A., Pokhilenko N. P., Golovin A. V., Cherepanova Y. and Sharygin I. S. (2013) Metasomatism in lithospheric mantle roots: Constraints from whole-rock and mineral chemical composition of deformed peridotite xenoliths from kimberlite pipe Udachnaya. *Lithos* **160–161**, 201–215.

Agashev A. M., Pokhilenko N. P., Tolstov A. V., Polyanichko V. V., Malkovets V. G. and Sobolev N. V. (2004) New age data on kimberlites from the Yakutian diamondiferous province. *Doklady Akad. Nauk SSSR Earth Sci. Sect.* **399**, 1142–1145.

Aulbach S., Mungall J. E. and Pearson D. G. (2016) Distribution and processing of highly siderophile elements in cratonic mantle lithosphere. *Rev. Miner. Geochem.* **81**, 239–304.

Blanco D., Kravchinsky V. A., Konstantinov K. M. and Kabin K. (2013) Paleomagnetic dating of Phanerozoic kimberlites in Siberia. *J. Appl. Geophys.* **88**, 139–153.

Bodinier J.-L., Garrido C. J., Chanefo I., Bruguier O. and Gervilla F. (2008) Origin of pyroxenite-peridotite veined mantle by refertilization reactions: evidence from the ronda peridotite (Southern Spain). *J. Petrol.* **49**, 999–1025.

Boyd F. R. (1989) Compositional distinction between oceanic and cratonic lithosphere. *Earth Planet. Sci. Lett.* **96**, 15–26.

Boyd F. R. and McCallister R. H. (1976) Densities of fertile and sterile garnet peridotites. *Geophys. Res. Lett.* **3**, 509–512.

Boyd F. R., Pokhilenko N. P., Pearson D. G., Mertzman S. A., Sobolev N. V. and Finger L. W. (1997) Composition of the Siberian cratonic mantle: evidence from Udachnaya peridotite xenoliths. *Contrib. Miner. Petrol.* **128**, 228–246.

Brey G., Brice W. R., Ellis D. J., Green D. H., Harris K. L. and Ryabchikov I. D. (1983) Pyroxene-carbonate reactions in the upper mantle. *Earth Planet. Sci. Lett.* **62**, 63–74.

Brey G. P. and Köhler T. (1990) Geothermobarometry in four-phase lherzolites II. New thermobarometers, and practical assessment of existing thermobarometers. *J. Petrol.* **31**, 1353–1378.

Bussweiler Y., Stone R. S., Pearson D. G., Luth R. W., Stachel T., Kjarsgaard B. A. and Menzies A. (2016) The evolution of calcite-bearing kimberlites by melt-rock reaction: evidence from polymineralic inclusions within clinopyroxene and garnet megacrysts from Lac de Gras kimberlites, Canada. *Contrib. Miner. Petrol.* **171**, 1–25.

Carlson R. W. (2005) Application of the Pt–Re–Os isotopic systems to mantle geochemistry and geochronology. *Lithos* **82**, 249–272.

Carlson R. W., Pearson D. G. and James D. E. (2005) Physical, chemical, and chronological characteristics of continental mantle. *Rev. Geophys.* **43**, RG1001.

Casagli A., Frezzotti M. L., Peccerillo A., Tiepolo M. and De Astis G. (2017) (Garnet)-spinel peridotite xenoliths from Mega (Ethiopia): evidence for rejuvenation and dynamic thinning of the lithosphere beneath the southern Main Ethiopian Rift. *Chem. Geol.* **455**, 231–248.

Chu Z.-Y., Wu F.-Y., Walker R. J., Rudnick R. L., Pitcher L., Puchtel I. S., Yang Y.-H. and Wilde S. A. (2009) Temporal evolution of the lithospheric mantle beneath the Eastern North China Craton. *J. Petrol.* **50**, 1857–1898.

Dalton J. A. and Presnall D. C. (1998) The continuum of primary carbonatitic-kimberlitic melt compositions in equilibrium with lherzolite: data from the system: CaO-MgO-Al_2O_3-SiO_2-CO_2 at 6 GPa. *J. Petrol.* **39**, 1953–1964.

Dalton J. A. and Wood B. J. (1993) The compositions of primary carbonate melts and their evolution through wallrock reaction in the mantle. *Earth Planet. Sci. Lett.* **119**, 511–525.

Dasgupta R., Hirschmann M. M., McDonough W. F., Spiegelman M. and Withers A. C. (2009) Trace element partitioning between garnet lherzolite and carbonatite at 6.6 and 8.6 GPa with applications to the geochemistry of the mantle and of mantle-derived melts. *Chem. Geol.* **262**, 57–77.

Davis G. L., Sobolev N. V. and Kharkiv A. D. (1980) New data on the age of Yakutian kimberlites from the U-Pb method on zircons. *Trans. (Doklady) Russ. Acad. Sci.* **254**, 175–179.

Dawson J. B. (1984) Contrasting types of upper-mantle metasomatism?. In *Kimberlites II. The Mantle and Crust-Mantle Relationships* (ed. J. Kornprobst). Elsevier Amsterdam, pp. 282–331.

Doucet L., Ionov D. and Golovin A. (2013) The origin of coarse garnet peridotites in cratonic lithosphere: new data on xenoliths from the Udachnaya kimberlite, central Siberia. *Contrib. Miner. Petrol.* **165**, 1225–1242.

Doucet L. S., Ionov D. A., Golovin A. V. and Pokhilenko N. P. (2012) Depth, degrees and tectonic settings of mantle melting during craton formation: inferences from major and trace element compositions of spinel harzburgite xenoliths from the Udachnaya kimberlite, central Siberia. *Earth Planet. Sci. Lett.* **359–360**, 206–218.

Elthon D. (1992) Chemical trends in abyssal peridotites: refertilization of depleted suboceanic mantle. *J. Geophys. Res.* **97**, 9015–9025.

Fan W. M., Zhang H. F., Baker J., Jarvis K. E., Mason P. R. D. and Menzies M. A. (2000) On and off the North China Craton: where is the Archaean keel? *J. Petrol.* **41**, 933–950.

Field S. W. and Haggerty S. E. (1994) Symplectites in upper mantle peridotites: development and implications for the growth of subsolidus garnet, pyroxene and spinel. *Contrib. Mineral. Petrol.* **118**, 138–156.

Foley S. F. (2008) Rejuvenation and erosion of the cratonic lithosphere. *Nat. Geosci.* **1**, 503–510.

Gaetani G. A., Kent A. J. R., Grove T. L., Hutcheon I. D. and Stolper E. M. (2003) Mineral/melt partitioning of trace elements during hydrous peridotite partial melting. *Contrib. Mineral. Petrol.* **145**, 391–405.

Gao S., Rudnick R. L., Carlson R. W., McDonough W. F. and Liu Y.-S. (2002) Re-Os evidence for replacement of ancient mantle lithosphere beneath the North China craton. *Earth Planet. Sci. Lett.* **198**, 307–322.

Gao S., Rudnick R. L., Xu W.-L., Yuan H.-L., Liu Y.-S., Walker R. J., Puchtel I. S., Liu X., Huang H., Wang X.-R. and Yang J. (2008) Recycling deep cratonic lithosphere and generation of intraplate magmatism in the North China Craton. *Earth Planet. Sci. Lett.* **270**, 41–53.

Gervasoni F., Klemme S., Rohrbach A., Grützner T. and Berndt J. (2017) Experimental constraints on mantle metasomatism caused by silicate and carbonate melts. *Lithos* **282–283**, 173–186.

Golovin A. V., Sharygin I. S. and Korsakov A. V. (2017) Origin of alkaline carbonates in kimberlites of the Siberian craton: evidence from melt inclusions in mantle olivine of the Udachnaya-East pipe. *Chem. Geol.* **455**, 357–375.

Goncharov A. G., Ionov D. A., Doucet L. S. and Pokhilenko L. N. (2012) Thermal state, oxygen fugacity and C-O-H fluid speciation in cratonic lithospheric mantle: new data on peridotite xenoliths from the Udachnaya kimberlite, Siberia. *Earth Planet. Sci. Lett.* **357–358**, 99–110.

Green D. H. and Wallace M. E. (1988) Mantle metasomatism by ephemeral carbonatite melts. *Nature* **336**, 459–462.

Griffin W. L., Ryan C. G., Kaminsky F. V., O'Reilly S. Y., Natapov L. M., Win T. T., Kinny P. D. and Ilupin I. P. (1999) The Siberian lithosphere traverse: mantle terranes and the assembly of the Siberian Craton. *Tectonophysics* **310**, 1–35.

Harte B. (1983) Mantle peridotites and processes – the kimberlite sample. In *Continental Basalts and Mantle Xenoliths* (eds. C. J. Hawkesworth and M. J. Norry). Shiva, Norwich, UK, pp. 46–91.

Hauri E. H., Shimizu N., Dieu J. J. and Hart S. R. (1993) Evidence for hotspot-related carbonatite metasomatism in the oceanic upper mantle. *Nature* **365**, 221–227.

Hellebrand E., Snow J. E., Hoppe P. and Hofmann A. W. (2002) Garnet-field melting and late-stage refertilization in 'residual' abyssal peridotites from the Central Indian Ridge. *J. Petrol.* **43**, 2305–2338.

Herzberg C. (2004) Geodynamic information in peridotite petrology. *J. Petrol.* **45**, 2507–2530.
Herzberg C., Condie K. and Korenaga J. (2010) Thermal history of the Earth and its petrological expression. *Earth Planet. Sci. Lett.* **292**, 79–88.
Herzberg C. and Rudnick R. (2012) Formation of cratonic lithosphere: an integrated thermal and petrological model. *Lithos* **149**, 4–15.
Howarth G. H., Barry P. H., Pernet-Fisher J. F., Baziotis I. P., Pokhilenko N. P., Pokhilenko L. N., Bodnar R. J., Taylor L. A. and Agashev A. M. (2014) Superplume metasomatism: evidence from Siberian mantle xenoliths. *Lithos* **184–187**, 209–224.
Humphreys E. D., Schmandt B., Bezada M. J. and Perry-Houts J. (2015) Recent craton growth by slab stacking beneath Wyoming. *Earth Planet. Sci. Lett.* **429**, 170–180.
Hunter R. H. and McKenzie D. (1989) The equilibrium geometry of carbonate melts in rocks of mantle composition. *Earth Planet. Sci. Lett.* **92**, 347–356.
Ionov D. A. (1998) Trace element composition of mantle-derived carbonates and coexisting phases in peridotite xenoliths from alkali basalts. *J. Petrol.* **39**, 1931–1941.
Ionov D. A. (2004) Chemical variations in peridotite xenoliths from Vitim, Siberia: inferences for REE and Hf behaviour in the garnet facies upper mantle. *J. Petrol.* **45**, 343–367.
Ionov D. A. (2007) Compositional variations and heterogeneity in fertile lithospheric mantle: peridotite xenoliths in basalts from Tariat, Mongolia. *Contrib. Mineral. Petrol.* **154**, 455–477.
Ionov D. A., Ashchepkov I. and Jagoutz E. (2005a) The provenance of fertile off-craton lithospheric mantle: Sr-Nd isotope and chemical composition of garnet and spinel peridotite xenoliths from Vitim, Siberia. *Chem. Geol.* **217**, 41–75.
Ionov D. A., Bodinier J.-L., Mukasa S. B. and Zanetti A. (2002) Mechanisms and sources of mantle metasomatism: major and trace element compositions of peridotite xenoliths from Spitsbergen in the context of numerical modeling. *J. Petrol.* **43**, 2219–2259.
Ionov D. A., Carlson R. W., Doucet L. S., Golovin A. V. and Oleinikov O. B. (2015a) The age and history of the lithospheric mantle of the Siberian craton: Re–Os and PGE study of peridotite xenoliths from the Obnazhennaya kimberlite. *Earth Planet. Sci. Lett.* **428**, 108–119.
Ionov D. A., Chanefo I. and Bodinier J.-L. (2005b) Origin of Fe-rich lherzolites and wehrlites from Tok, SE Siberia by reactive melt percolation in refractory mantle peridotites. *Contrib. Miner. Petrol.* **150**, 335–353.
Ionov D. A., Chazot G., Chauvel C., Merlet C. and Bodinier J.-L. (2006a) Trace element distribution in peridotite xenoliths from Tok, SE Siberian craton: a record of pervasive, multi-stage metasomatism in shallow refractory mantle. *Geochim. Cosmochim. Acta* **70**, 1231–1260.
Ionov D. A., Doucet L. S. and Ashchepkov I. V. (2010) Composition of the lithospheric mantle in the Siberian craton: new constraints from fresh peridotites in the Udachnaya-East kimberlite. *J. Petrol.* **51**, 2177–2210.
Ionov D. A., Doucet L. S., Carlson R. W., Golovin A. V. and Korsakov A. V. (2015b) Post-Archean formation of the lithospheric mantle in the central Siberian craton: Re–Os and PGE study of peridotite xenoliths from the Udachnaya kimberlite. *Geochim. Cosmochim. Acta* **165**, 466–483.
Ionov D. A., Doucet L. S., Pogge von Strandmann P. A. E., Golovin A. V. and Korsakov A. V. (2017) Links between deformation, chemical enrichments and Li-isotope compositions in the lithospheric mantle of the central Siberian craton. *Chem. Geol.* **475**, 105–121.
Ionov D. A., Dupuy C., O'Reilly S. Y., Kopylova M. G. and Genshaft Y. S. (1993) Carbonated peridotite xenoliths from Spitsbergen: implications for trace element signature of mantle carbonate metasomatism. *Earth Planet. Sci. Lett.* **119**, 283–297.
Ionov D. A. and Hofmann A. W. (2007) Depth of formation of sub-continental off-craton peridotites. *Earth Planet. Sci. Lett.* **261**, 620–634.
Ionov D. A., O'Reilly S. Y. and Griffin W. L. (1997) Volatile-bearing minerals and lithophile trace elements in the upper mantle. *Chem. Geol.* **141**, 153–184.
Ionov D. A., O'Reilly S. Y., Kopylova M. G. and Genshaft Y. S. (1996) Carbonate-bearing mantle peridotite xenoliths from Spitsbergen: phase relationships, mineral compositions and trace element residence. *Contrib. Mineral. Petrol.* **125**, 375–392.
Ionov D. A., Prikhodko V. S., Bodinier J.-L., Sobolev A. V. and Weis D. (2005c) Lithospheric mantle beneath the south-eastern Siberian craton: petrology of peridotite xenoliths in basalts from the Tokinsky Stanovik. *Contrib. Miner. Petrol.* **149**, 647–665.
Ionov D. A., Savoyant L. and Dupuy C. (1992) Application of the ICP-MS technique to trace element analysis of peridotites and their minerals. *Geostandard. Newsl.* **16**, 311–315.
Ionov D. A., Shirey S. B., Weis D. and Brügmann G. (2006b) Os-Hf-Sr-Nd isotope and PGE systematics of spinel peridotite xenoliths from Tok, SE Siberian craton: effects of pervasive metasomatism in shallow refractory mantle. *Earth Planet. Sci. Lett.* **241**, 47–64.
Kelemen P. B. (1990) Reaction between ultramafic wall rock and fractionating basaltic magma: Part I – Phase relations, the origin of calc-alkaline magma series, and the formation of discordant dunite. *J. Petrol.* **31**, 51–98.
Kelemen P. B., Dick H. J. and Quick J. E. (1992) Formation of harzburgite by pervasive melt/rock reaction in the upper mantle. *Nature* **358**, 635–641.
Kinny P. D., Griffin B. J., Heaman L. M., Brakhfogel F. F. and Spetsius Z. V. (1997) SHRIMP U-Pb ages of perovskite from Yakutian kimberlites. *Geol. Geofiz.* **38**, 91–99 (in Russian).
Kostrovitsky S. I., Skuzovatov S. Y., Yakovlev D. A., Sun J., Nasdala L. and Wu F.-Y. (2016) Age of the Siberian craton crust beneath the northern kimberlite fields: insights to the craton evolution. *Gondwana Res.* **39**, 365–385.
Lee C.-T., Rudnick R. L., McDonough W. F. and Horn I. (2000) Petrologic and geochemical investigation of carbonates in peridotite xenoliths from northeastern Tanzania. *Contrib. Mineral. Petrol.* **139**, 470–484.
Liu J., Riches A. J. V., Pearson D. G., Luo Y., Kienlen B., Kjarsgaard B. A., Stachel T. and Armstrong J. P. (2016) Age and evolution of the deep continental root beneath the central Rae craton, northern Canada. *Precambrian Res.* **272**, 168–184.
McDonough W. F. and Sun S.-S. (1995) The composition of the Earth. *Chem. Geol.* **120**, 223–253.
Meisel T., Walker R. J., Irving A. J. and Lorand J.-P. (2001) Osmium isotopic compositions of mantle xenoliths: a global perspective. *Geochim. Cosmochim. Acta* **65**, 1311–1323.
Mercier J.-C. C. and Nicolas A. (1975) Textures and fabrics of upper mantle peridotites as illustrated by xenoliths from basalts. *J. Petrol.* **16**, 454–487.
Merlet C. (1994) An accurate computer correction program for quantitative electron probe microanalysis. *Mikrochim. Acta* **114** (115), 363–376.
Mitchell A. L. and Grove T. L. (2016) Experiments on melt–rock reaction in the shallow mantle wedge. *Contrib. Miner. Petrol.* **171**, 107.
Morgan Z. and Liang Y. (2005) An experimental study of the kinetics of lherzolite reactive dissolution with applications to melt channel formation. *Contrib. Mineral. Petrol.* **150**, 369–385.
Moyen J.-F., Paquette J. L., Ionov D. A., Gannoun A., Korsakov A. V., Golovin A. V. and Moine B. N. (2017) Paleoproterozoic

rejuvenation and replacement of Archaean lithosphere: evidence from zircon U-Pb dating and Hf isotopes in crustal xenoliths at Udachnaya, Siberian craton. *Earth Planet. Sci. Lett.* **457**, 149–159.

Neumann E.-R., Wulff-Pedersen E., Pearson N. J. and Spenser E. A. (2002) Mantle xenoliths from Tenerife (Canary Islands): evidence for reactions between mantle peridotites and silicic carbonatite melts inducing Ca metasomatism. *J. Petrol.* **43**, 825–857.

Nickel K. G. and Green D. H. (1985) Empirical geothermobarometry for garnet peridotites and implications for the nature of the lithosphere, kimberlites and diamonds. *Earth Planet. Sci. Lett.* **73**, 158–170.

Nimis P. and Grütter H. (2010) Internally consistent geothermometers for garnet peridotites and pyroxenites. *Contrib. Miner. Petrol.* **159**, 411–427.

Paquette J. L., Ionov D. A., Agashev A. M., Gannoun A. and Nikolenko E. I. (2017) Age, provenance and Precambrian evolution of the Anabar shield from U-Pb and Lu-Hf isotope data on detrital zircons, and the history of the northern and central Siberian craton. *Precambrian Res.* **301**, 134–144.

Pearce N. J. G., Perkins W. T., Westgate J. A., Gorton M. P., Jackson S. E., Neal S. R. and Chenery S. P. (1997) A compilation of new and published major and trace element data for NIST SRM 610 and NIST SRM 612 glass reference materials. *Geostandard. Newsl.* **21**, 115–144.

Pearson D. G., Canil D. and Shirey S. B. (2014) Mantle samples included in volcanic rocks: xenoliths and diamonds. In *Treatise on Geochemistry* (ed. R. W. Carlson), second ed. Elsevier, Oxford, pp. 169–253.

Pearson D. G., Irvine G. J., Ionov D. A., Boyd F. R. and Dreibus G. E. (2004) Re-Os isotope systematics and platinum group element fractionation during mantle melt extraction: a study of massif and xenolith peridotite suites. *Chem. Geol.* **208**, 29–59.

Pearson D. G. and Wittig N. (2008) Formation of Archaean continental lithosphere and its diamonds: the root of the problem. *J. Geol. Soc. Lond.* **165**, 895–914.

Pearson D. G. and Wittig N. (2014) *The Formation and Evolution of Cratonic Mantle Lithosphere – Evidence from Mantle Xenoliths, Treatise on Geochemistry*, second ed. Elsevier, Oxford, pp. 255–292.

Pernet-Fisher J. F., Howarth G. H., Pearson D. G., Woodland S., Barry P. H., Pokhilenko N. P., Pokhilenko L. N., Agashev A. M. and Taylor L. A. (2015) Plume impingement on the Siberian SCLM: evidence from Re–Os isotope systematics. *Lithos* **218–219**, 141–154.

Press S., Witt G., Seck H. A., Eonov D. and Kovalenko V. I. (1986) Spinel peridotite xenoliths from the Tariat Depression, Mongolia. I: Major element chemistry and mineralogy of a primitive mantle xenolith suite. *Geochim. Cosmochim. Acta* **50**, 2587–2599.

Rehfeldt T., Foley S. F., Jacob D. E., Carlson R. W. and Lowry D. (2008) Contrasting types of metasomatism in dunite, wehrlite and websterite xenoliths from Kimberley, South Africa. *Geochim. Cosmochim. Acta* **72**, 5722–5756.

Rudnick R. L., Gao S., Ling W.-L., Liu Y.-S. and McDonough W. F. (2004) Petrology and geochemistry of spinel peridotite xenoliths from Hannuoba and Qixia, North China craton. *Lithos* **77**, 609–637.

Rudnick R. L., McDonough W. F. and Chappell B. C. (1993) Carbonatite metasomatism in the northern Tanzanian mantle. *Earth Planet. Sci. Lett.* **114**, 463–475.

Rudnick R. L. and Walker R. J. (2009) Interpreting ages from Re–Os isotopes in peridotites. *Lithos* **112**(Suppl. 2), 1083–1095.

Salters V. J. M. and Stracke A. (2004) Composition of the depleted mantle. *Geochem. Geophys. Geosyst.* **5**, Q05004.

Smith D. (1987) Genesis of carbonate in pyrope from ultramafic diatremes on the Colorado Plateau, southwestern US. *Contrib. Mineral. Petrol.* **97**, 389–396.

Snyder D. B., Humphreys E. and Pearson D. G. (2017) Construction and destruction of some North American cratons. *Tectonophysics* **694**, 464–485.

Snyder G. A., Taylor L. A., Crozaz G., Halliday A., Beard B. L., Sobolev V. N. and Sobolev N. V. (1997) The origins of Yakutian eclogite xenoliths. *J. Petrol.* **38**, 85–113.

Sobolev N. V. (1977) *Deep-Seated Inclusions in Kimberlites and the Problem of the Composition of the Upper Mantle*. American Geophysical Union, Washington, D.C..

Spetsius Z. V. and Serenko V. P. (1990) *Composition of the continental upper mantle and lower crust beneath the Siberian Platform*. Nauka, Moscow.

Streckeisen A. (1976) To each plutonic rock its proper name. *Earth Sci. Rev.* **12**, 1–33.

Sun J., Liu C.-Z., Tappe S., Kostrovitsky S. I., Wu F.-Y., Yakovlev D., Yang Y.-H. and Yang J.-H. (2014) Repeated kimberlite magmatism beneath Yakutia and its relationship to Siberian flood volcanism: insights from in situ U-Pb and Sr–Nd perovskite isotope analysis. *Earth Planet. Sci. Lett.* **404**, 283–295.

Takahashi N., Frey F. A., Shimizu N., Obata M. and Bodinier J. L. (1992) Geochemical evidence for melt migration and reaction in the upper mantle. *Nature* **359**, 55.

Takazawa E., Frey F. A., Shimizu N. and Obata M. (2000) Whole rock compositional variations in an upper mantle peridotite (Horoman, Hokkaido, Japan): are they consistent with a partial melting process. *Geochim. Cosmochim. Acta* **64**, 695–716.

Tang Y.-J., Zhang H.-F., Ying J.-F. and Su B.-X. (2013) Widespread refertilization of cratonic and circum-cratonic lithospheric mantle. *Earth Sci. Rev.* **118**, 45–68.

Taylor L. A., Snyder G. A., Keller R., Remley D. A., Anand M., Wiesli R., Valley J. and Sobolev N. V. (2003) Petrogenesis of group-A eclogites and websterites: evidence from the Obnazhennaya kimberlite, Yakutia. *Contrib. Mineral. Petrol.* **145**, 424–443.

Tursack E. and Liang Y. (2012) A comparative study of melt-rock reactions in the mantle: laboratory dissolution experiments and geological field observations. *Contrib. Miner. Petrol.* **163**, 861–876.

Ukhanov A. B., Ryabchikov I. D. and Kharkiv A. D. (1988) *Lithospheric Mantle of the Yakutian Kimberlite Province*. Nauka, Moscow.

van Achterbergh E., Ryan C., Jackson S. and Griffin W. (2001) Data reduction software for LA-ICP-MS. In *Laser Ablation-ICPMS in the Earth Science* (ed. P. Sylvester). Mineral. Assoc., Canada, pp. 239–243.

Walter M. J. (1999) Melting residues of fertile peridotite and the origin of cratonic lithosphere. In: Mantle Petrology: Field Observations and High-Pressure Experimentation. Spec. Publ. Geochem. (eds. Y. Fei, C. M. Bertka, B. O. Mysen). Soc. No. 6 Geochemical Society, Houston. pp. 225–239.

Walter M. J. (2003) Melt extraction and compositional variability in mantle lithosphere. In *Treatise on Geochemistry*, vol. 2 (ed. R. W. Carlson), pp. 363–394. The Mantle and Core. Elsevier, Amsterdam.

Wang C., Liang Y., Dygert N. and Xu W. (2016) Formation of orthopyroxenite by reaction between peridotite and hydrous basaltic melt: an experimental study. *Contrib. Miner. Petrol.* **171**, 1–18.

Wang H., van Hunen J. and Pearson D. G. (2015) The thinning of subcontinental lithosphere: the roles of plume impact and metasomatic weakening. *Geochem. Geophys. Geosyst.* **16**, 1156–1171.

Wiechert U., Ionov D. A. and Wedepohl K. H. (1997) Spinel peridotite xenoliths from the Atsagin-Dush volcano, Dariganga lava plateau, Mongolia: a record of partial melting and cryptic metasomatism in the upper mantle. *Contrib. Mineral. Petrol.* **126**, 345–364.

Wölbern I., Rümpker G., Link K. and Sodoudi F. (2012) Melt infiltration of the lower lithosphere beneath the Tanzania craton and the Albertine rift inferred from S receiver functions. *Geochem. Geophys. Geosyst.* **13**, Q0AK08.

Xu Y. (2001) Thermo-tectonic destruction of the Archaean lithospheric keel beneath the Sino-Korean craton in China: evidence, timing and mechanism. *Phys. Chem. Earth (A)* **26**, 747–757.

Yaxley G. M., Crawford A. J. and Green D. H. (1991) Evidence for carbonatite metasomatism in spinel peridotite xenoliths from western Victoria, Australia. *Earth Planet. Sci. Lett.* **107**, 305–317.

Yaxley G. M., Green D. H. and Kamenetsky V. (1998) Carbonate metasomatism in the southeastern Australian lithosphere. *J. Petrol.* **39**, 1917–1931.

Zhang H.-F., Goldstein S., Zhou X.-H., Sun M., Zheng J.-P. and Cai Y. (2008) Evolution of subcontinental lithospheric mantle beneath eastern China: Re–Os isotopic evidence from mantle xenoliths in Paleozoic kimberlites and Mesozoic basalts. *Contrib. Miner. Petrol.* **155**, 271–293.

Ziberna L., Klemme S. and Nimis P. (2013) Garnet and spinel in fertile and depleted mantle: insights from thermodynamic modelling. *Contrib. Miner. Petrol.* **166**, 411–421.

Associate Editor: Mark Rehkamper